

**AUTOMATIC BLOB-BASED GLISTENING DETECTION
IN INTRAOCULAR LENS**

BY

TEERANOOT JAPUNYA

**A THESIS SUBMITTED IN PARTIAL FULFILLMENT OF
THE REQUIREMENTS FOR THE DEGREE OF MASTER OF
ENGINEERING (INFORMATION AND COMMUNICATION
TECHNOLOGY FOR EMBEDDED SYSTEMS)
SIRINDHORN INTERNATIONAL INSTITUTE OF TECHNOLOGY
THAMMASAT UNIVERSITY
ACADEMIC YEAR 2015**

**AUTOMATIC BLOB-BASED GLISTENING DETECTION
IN INTRAOCULAR LENS**

BY

TEERANOOT JAPUNYA

**A THESIS SUBMITTED IN PARTIAL FULFILLMENT OF
THE REQUIREMENTS FOR THE DEGREE OF MASTER OF
ENGINEERING (INFORMATION AND COMMUNICATION
TECHNOLOGY FOR EMBEDDED SYSTEMS)**

SIRINDHORN INTERNATIONAL INSTITUTE OF TECHNOLOGY

THAMMASAT UNIVERSITY

ACADEMIC YEAR 2015



AUTOMATIC BLOB-BASED GLISTENING DETECTION IN INTRAOCULAR LENS

A Thesis Presented

By

TEERANOOT JAPUNYA

Submitted to

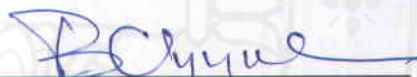
Sirindhorn International Institute of Technology

Thammasat University

In partial fulfillment of the requirements for the degree of
MASTER OF ENGINEERING (INFORMATION AND COMMUNICATION
TECHNOLOGY FOR EMBEDDED SYSTEMS)

Approved as to style and content by

Advisor and Chairperson of Thesis Committee



(Assoc. Prof. Bunyarit Uyyanonvara, Ph.D)

Committee Member and
Chairperson of Examination Committee



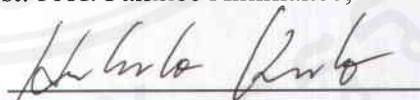
(Chanjira Sinthanayothin, Ph.D)

Committee Member



(Asst. Prof. Pakinee Aimmanee, Ph.D)

Committee Member



(Assoc. Prof. Hirohiko Kaneko, Ph.D)

November 2015

Acknowledgements

I am using this opportunity to express my sincere gratitude and gratefully all those who made this dissertation possible to complete.

My deepest gratitude is to my advisor, Assoc. Prof. Dr. Bunyarit Uyyanonvara. He has been supportive since the day we met. He is the funniest advisor and one of the smartest people I know. The major successful of this thesis comes from his excellent guidance, caring, patience and supportive for doing the research.

I acknowledge my gratitude to Dr. Chanjira Sinthanayothin, Asst. Prof. Dr. Pakinee Aimmanee and Prof. Hirohiko Kaneko for insightful guideline, comments and questions. Those words helped me to improve the method.

I am indebted to Miss Parisut Jitpakdee for starting this research and teaching a lot of knowledge in image processing field.

I also thank my ICTES#6 friends, Chatpadol Klungmontri, Sattakan Thananchai, Vasiophon Pawankiattikun, Arthit Julkananusart, Wichai Treethidtaphat, Pongsate Tangseg, and Thanapha Chantharaphaichit who friendly support and give motivation to complete this research. They always help me to solve problems when I need it.

Winit Preechaphakorn, Tu Anh Nguyen and Somphon Tripan are lovely friends who always beside me. Thank you for understanding me and always listen my problems although you don't know about my research.

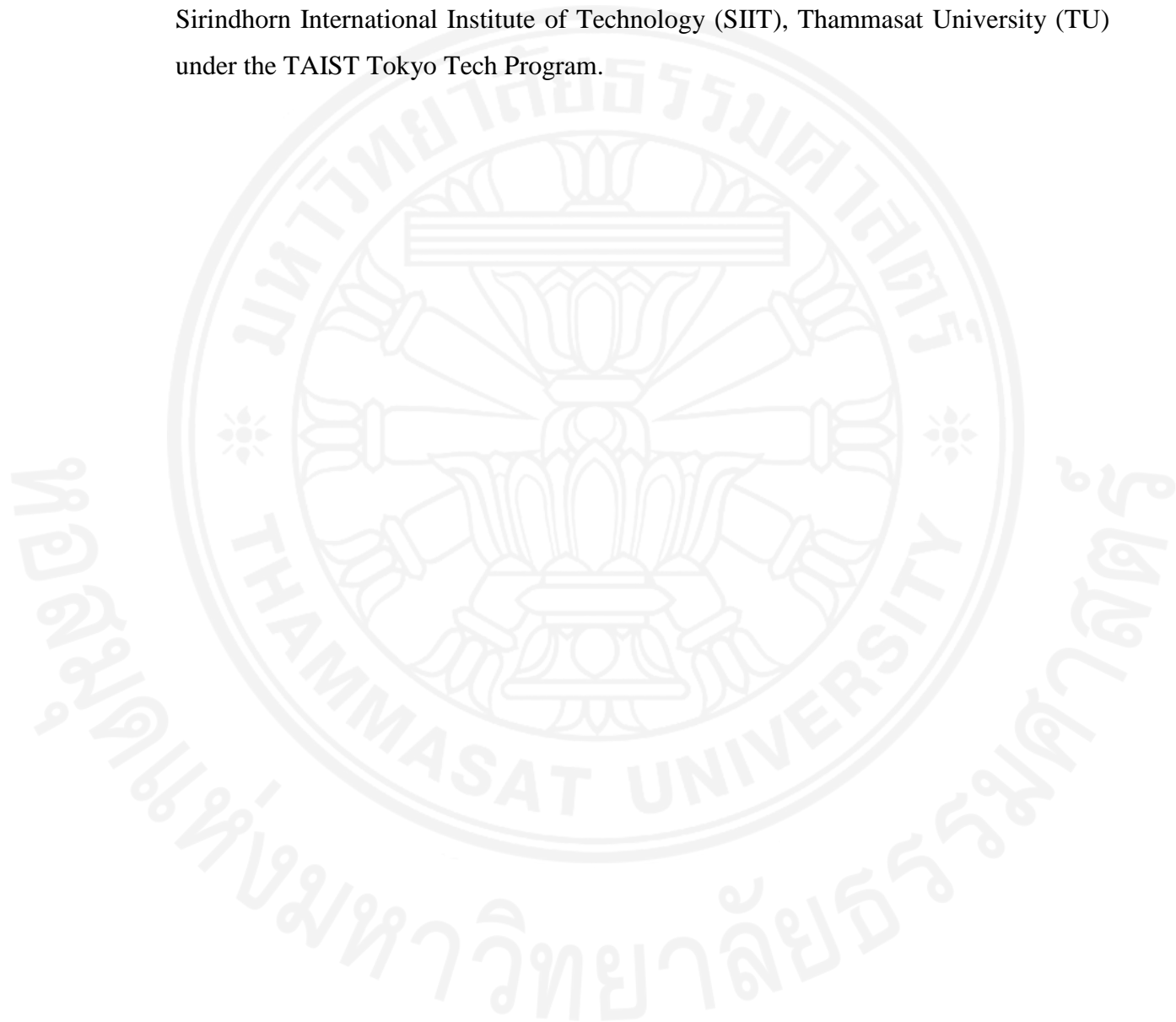
Truc Giang have taught English for me. I appreciate for your kind teaching. My English skill is improved because of you.

My very sincere thanks to The Applied Vision Research Centre, School of Health Sciences, City University London, Especially Eva Philippaki, Chris Hull, and Sarah Barman for The Intraocular lens images and ground truth data.

This thesis would not have been possible without my parents' support. I would like to thank you for supporting me and allow me to take this program. Thank you for believing in me and taught me to believing in myself.

Last but not least, Thank you for Laboratory of Information Communication Networks, Hokkaido University. Atmospheres in the lab farce me to start writing this thesis and finish it faster than I expect.

This work was supported in part by the National Research University Project of Thailand Office of Higher Education Commission (Thammasat University), Thailand Advanced Institute of Science and Technology (TAIST), National Science and Technology Development Agency (NSTDA), Tokyo Institute of Technology, and Sirindhorn International Institute of Technology (SIIT), Thammasat University (TU) under the TAIST Tokyo Tech Program.



Abstract

AUTOMATIC BLOB-BASED GLISTENING DETECTION IN INTRAOCULAR LENS

by

TEERANOOT JAPUNYA

Bachelor of Engineering in Computer Engineering, Faculty of Engineering, Thai-Nichi Institute of Technology, 2012

An intraocular lens (IOL) is implanted in the eye after a cataract surgery. When an IOL is in an aqueous environment, glistenings that are fluid-filled microvacuoles are often observed. Glistenings appear like sesame or bubble in IOL lens. It can effect human vision by increasing forward light scatter. Previously, studies of glistenings involved tedious work of manual glistenings labeling and rough estimation of glistening distribution. This thesis have studied about the automatic glistening detection in intraocular lens using MATLAB. The detection algorithm is applied by blob detection and exudate detection. It also using Watershed algorithm to increase detection performance by separate closed, touched and overlapped glistening. We have developed software which has a user friendly for who have no knowledge about MATLAB and Image processing. After get important data includes maximum glistening area, minimum glistening area, maximum threshold value, minimum threshold value, step threshold value and lens mark, the software computes and displays important properties such as average glistening area and distribution of glistening for user. The result shows that the proposed method can efficiently detected glistening.

Keywords: Glistening Detection, Medical Image Processing, Watershed Algorithm, Intraocular lens

Table of Contents

Chapter	Title	Page
	Signature Page	i
	Acknowledgements	ii
	Abstract	iv
	Table of Contents	v
	List of Figures	viii
	List of Tables	x
1	Introduction	1
	1.1 Glistening	1
	1.2 Motivation	2
	1.3 Objectives	3
	1.4 Thesis structure	4
2	Literature Review	5
	2.1 Glistening and surface light scattering in intraocular lenses	5
	2.2 Blob detection	6
	2.3 Exudate detection	7
	2.4 Drusen	8
	2.5 Watershed Algorithm	9
3	Automatic blob-based glistening detection in intraocular lens	12
	3.1 Introduction	12

3.2 Software for the Quantification of Glistenings in Intra-Ocular Lenses	12
(a) IOL image selection and display	13
(b) Lens Detection	13
(c) Glistening Detection	14
(d) Ground truth Selection (for development phase)	14
(e) Layer Selection	14
(f) Image Saving	14
(g) Quantification results	14
(h) Validation result	14
3.3 Glistening detection algorithm	15
(a) Pre-processing	15
(b) Edge Detection	17
(c) Connect broken lines and fill holes	20
(d) Border Hardening	26
(e) Candidate Classification	29
(f) Candidate Selection	29
3.4 Conclusion	30
4 Quantification of the Overlapped glistening in Intra-Ocular lens	33
4.1 Introduction	33
4.2 Glistening separation process	34
(a) Pre-processing	34
(b) Foreground extraction	34
(c) Watershed Algorithm	35
(d) Combine result	36
4.3 Conclusion	37
5 Evaluation and Result Discussion	41
5.1 Experimental Data	41

5.2 Evaluation	43
5.2.1 Accuracy and Sensitivity	43
5.2.2 Number of Glistening	45
5.3 Conclusion	49
6 Conclusion and Recommendations	50
6.1 Research Summary	50
6.2 Key Contributions of this Research	50
6.3 Future Study	50
References	52
Appendix A	56

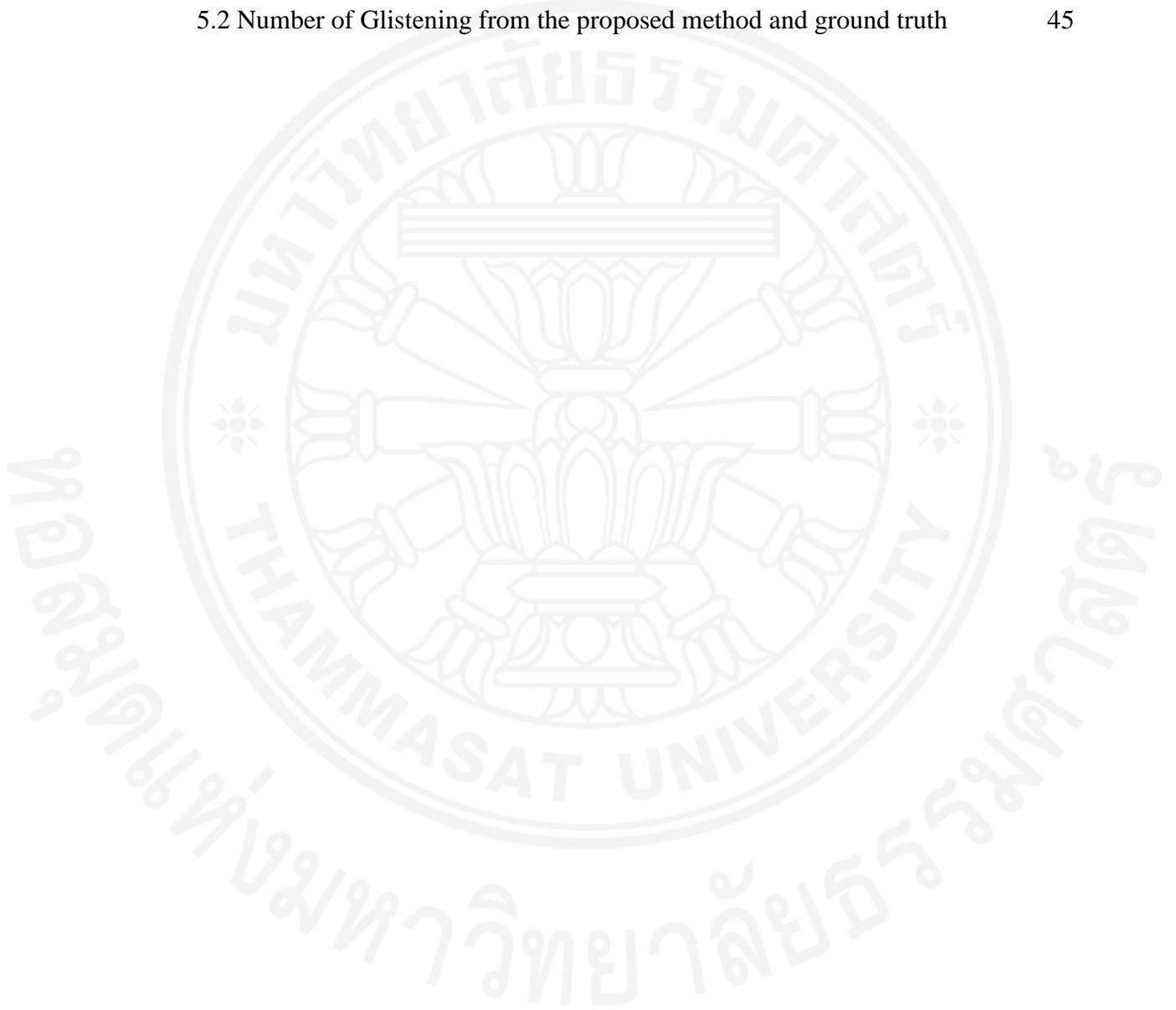
List of Figures

Figures	Page
1.1 IOL lens image with glistenings	2
2.1 One-piece foldable hydrophobic acrylic IOL	6
2.2 Image with hard exudates	8
2.3 Normal and Abnormal Retinal images	9
2.4 Example Image of Watershed algorithm	10
2.5 Image of Marker-Controlled Watershed algorithm result	11
3.1 Screen of software shows the comparison of detected glistenings and the ground truth	13
3.2 Flow chart of glistening detection method	15
3.3 Comparison of Original image and Red, Green, Blue channel extraction (set 1)	16
3.4 Comparison of Original image and Red, Green, Blue channel extraction (set 2)	17
3.5 Comparison of Original image and Red, Green, Blue channel extraction (set 3)	18
3.6 Edge detection result (set 1)	19
3.7 Edge detection result (set 2)	20
3.8 Sobel operation result with difference threshold value (set 1)	21
3.9 Sobel operation result with difference threshold value (set 2)	22
3.10 Mask for dilation and erosion operation	23
3.11 Example of connect broken line and fill holes step (set 1)	24
3.12 Example of connect broken line and fill holes step (set 2)	25
3.13 Example of border hardening step (set 1)	27
3.14 Example of border hardening step (set 2)	28
3.15 Candidate classification result	29
3.16 Candidate classification result in different threshold value (set 1)	30
3.17 Candidate classification result in different threshold value (set 2)	31
3.18 Glistening algorithm result	32
4.1 Glistening separation flowchart	34

4.2 Example when Otsu thresholding method difference detected	35
4.3 Example of watershed result of IOL image	36
4.4 Example of final result of Glistening separation algorithm (set 1)	38
4.5 Example of final result of Glistening separation algorithm (set 2)	39
4.6 Example of final result of Glistening separation algorithm (set 3)	40
5.1 Several images of IOL input image	42
5.2 Example of the ground truth image	43
5.2 Example of the IOL lens which hard to count glistening with human eye	45

List of Tables

Tables	Page
5.1 Result of Glistening detection and variable data for each image	44
5.2 Number of Glistening from the proposed method and ground truth	45



Chapter 1

Introduction

Glistenings are fluid-filled microvacuoles that form within the IOL lens. The common way to quantify the glistening is to identify each clinical glistening's significance manually. However, this way is time-consuming to finish each IOL image. Once IOL image consists of hundreds of glistening in difference size. It is difficult to quantify glistening in one lens and calculate the size of glistening. In this research, we tried to solve this problem by using Image processing technique to quantification glistening in an Intraocular lens. Glistening appears like a bubble or sesame in IOL lens. It can be detected apply by blob and exudate detection. The high performance of glistening detection is required correctly detected result for assign appropriate treatment. In this chapter, glistening is introduced for the background knowledge. Motivation and Objectives are described briefly. Finally, Thesis structure is presented for reviewed the overall of this thesis.

1.1 Glistening

An intraocular lens (IOL) is a lens implanted in the eye to replace the crystalline lens of the human eye after cataract or refractive lens surgery [1]. It's common type is inserted into the capsular bag of the eye [1]. Many research has shown if the IOL is in an aqueous environment, fluid-filled microvacuoles are formed within an IOL, called glistenings [2, 3, 4, 5, 6]. The most studies described for the formation of glistenings theory is that polymers absorb water when immersed in an aqueous environment over an extended period of time and that if the water vapor detaches from its surrounding matter and gathers into a void within the polymer network of the IOL, glistening forms[4]. However, they have been appeared in various IOL materials such as silicone, hydrogel, and poly (methyl methacrylate) (PMMA) [2]. Some study describes time after cataract surgery is the most significant influence on glistening formation [2, 3, 4] although there is difference time that glistenings were observed after surgery [2]. Other factors influencing glistening formation include changes in temperature, IOL manufacturing, packaging techniques, IOL material composition and associated condition such as glaucoma. Fig. 1 Shows the IOL image example

with glistenings. Normally, Glistenings appear like bubble or sesame in IOL lens. It has difference colors.

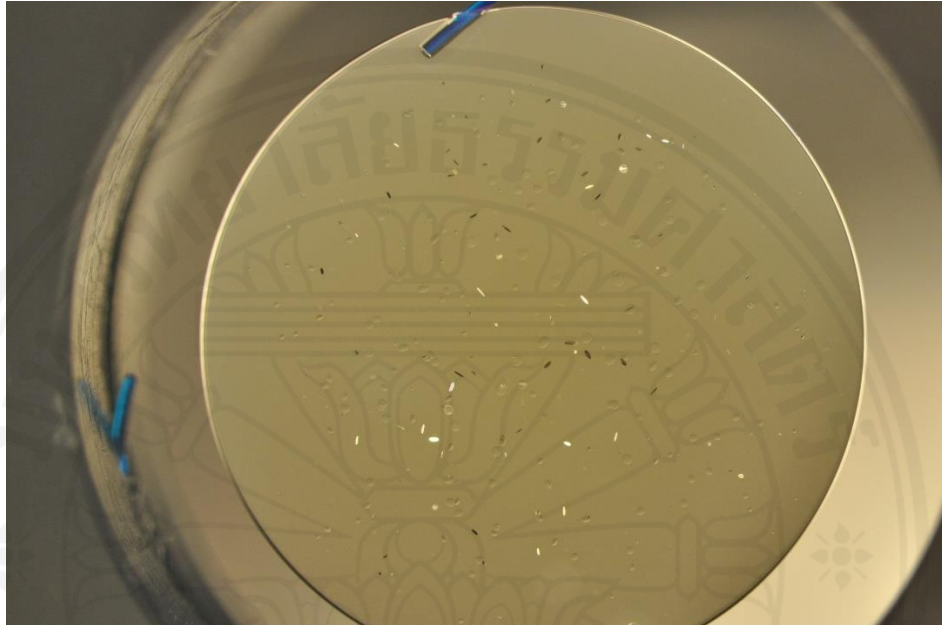


Fig. 1.1 IOL lens image with glistenings [Taken from: The Applied Vision Research Centre, School of Health Sciences, City University London]

1.2 Motivation

Glistenings, fluid-filled microvacuoles, are formed within an IOL, when the IOL lens is in an aqueous environment. Glistenings can affect human vision by increasing forward light scatter [7, 8, 9]. An effect is varying by the difference of size, density and location of glistenings [10]. A few studies suggest other groups look for the glistening detection using image processing technique [11]. However, there is no specific method to detecting glistening. Glistening quantification is required to assess the quality of the lens and also to assign appropriate treatment. Due to the size of the lens, it is difficult to get a good quality image of all IOL lens.

Blob detection is the technique to detect brighter or darker region compared with the surrounding area or in the same color in the image or video [12, 13]. Basically, a blob can be detected by thresholding the image, or its bounds can be defined by edge filter [14]. The leakage of proteins and lipid from the bloodstream into the retina via damaged blood vessels, called exudate [15, 16]. Hard exudates are

shown as bright yellow lesions with varying sizes, shapes, and locations in the retinal image [16].

Blob and Exudate detection can apply for glistening detection. Both techniques provide high performance for glistening detection. This study mainly focuses on developing software for the Quantification of Glistenings in Intra-Ocular Lenses. The software has a user-friendly front-end and is designed to semi-automatically detect glistenings. Once detected, the software computes and displays important properties for the user. Its GUI is designed for the convenience of users who are typically clinicians or scientists with little image processing knowledge.

1.3 Objectives

The objective of this study is to develop a novel technique for glistening detection base on blob and exudate detection. This technique is used in glistening quantification software which is designed for the convenience of users who are typically clinicians or scientists with little image processing knowledge.

The objectives and scope of this research are as follows;

1. Research on blob and exudate detection to apply for glistening detection.
2. Develop an image processing technique of glistening detection based on Blob and exudate detection.
3. Develop an image processing technique of separating glistening based on Watershed algorithm.
4. Design glistening quantification software that has a user-friendly front-end.

1.4 Thesis Structure

This thesis provides descriptions of glistening detection in difference ways.

Chapter 1 – *Introduction* explains a brief introduction of this study along with motivation and the objective.

Chapter 2 – *Background and Literature Review* describes the background of blob and exudate detection. Watershed algorithm is also explained, focusing on the image processing technique.

Chapter 3 – *Automatic blob-based Glistening Detection* presents a novel method for glistening detection base on blob and exudate detection. Software for the quantification of glistenings is also presented.

Chapter 4 – *Quantification of the overlapped glistening in intraocular lens* describes the novel method applied from watershed algorithm to separate glistening. This chapter explain the merit and demerit of this method.

Chapter 5 – *Evaluation* proposes a result of glistening detection comparing with the ground truth.

Chapter 6 – *Discussions and Conclusions* discusses on the brief conclusion and future work of this study.

Chapter 2

Literature Review

This chapter aims to explain about glistening information such as its theory, factors, etc. Next, the related technique which can apply to detect glistening will be reviewed. Blob detection is applied to detect glistening because glistening appears like blobs in IOL lens. Exudate, ROP and drusen detection are the human eye problems. Those techniques can be developed for the glistening detection. Finally, the watershed algorithm is reviewed. It is the basically image segmentation approach that we can use for glistening segmentation algorithm.

2.1 Glistening and surface light scattering in intraocular lenses

Liliana Wener [2] has study about glistening, a fluid-filled microvacuoles that form within the IOL optic when IOL is in an aqueous environment. Glistening is described that it association with hydrophobic acrylic IOLs. The most studies described for the formation of glistenings theory is that polymers absorb water when immersed in an aqueous environment over an extended period of time and that if the water vapor detaches from its surrounding matter and gathers into a void within the polymer network of the IOL, glistening forms [2-4]. The time of onset was as early as 1 week after the operation while some case, glistenings were not observed up to 6 months postoperative. Some research [2, 3, 4] describe that the most significant influence on glistening formation is the time after cataract surgery. However, factors of glistening formation include temperature changes, IOL manufacturing, packaging techniques, IOL material composition and associated condition such as glaucoma. Glistenings can be observed throughout the entire IOL lens [2]. The degree of glistenings are different in each eye [2]. Subjective/semiquantitative grading of density assessed at the slitlamp and slitlamp photography of the IOL at high magnification with quantification of the size and number of glistenings manually or image analysis can be used for grading glistenings [2]. To quantify glistening, Klos et al [2, 17] suggested that Scheimpflug photography could be used as different types of irregularities, damage, or disturbances in transparency of the IOL material could be identified by more or less intensive light scattering.

Glistenings distribute in several size. The common size of glistening observed in clinically or induced in a laboratory setting by immersing the IOLs in water and submitting them to fluctuations in the temperature range from 1 to 20 μm . It usually observed up to 10 μm in diameter [2].

Fig 2.1 presents the example image of Hydrophobic acrylic IOLs lens.



Fig. 2.1 One-piece foldable hydrophobic acrylic IOL. [1]

2.2 Blob detection

Blob detection, an important low-level operation in computer vision, is usually a first step toward more complicated tasks [17]. Basically, blob detection is used for segmenting the interested object from the background. Blob is defined as a compact region lighter (or darker) than its background surrounded by smoothly curved edge [18]. In principle, blobs can be segmented by thresholding the image at an appropriate level, or its boundaries can be defined by an edge detector [14].

Krit I. et. al.[19] have proposed blob detection methods with feature stability along with the use of KNN algorithm. They constructed scale-space tree based on the blobs that were created from a series of images after blurring with Gaussian kernel. Feature stability used for demonstrates the blob linking process while blobs are represented as a node. A user can determine the type of blobs that were detected within the image by distinguishing classes to create ground truth images. KNN algorithm is applied to processed and compared for the algorithm's effectiveness in the same process.

Christophe D. and Sylvain M. [17] had proposed a novel method to detecting blob based on wavelet transform modulus maxima. They have considered modulus maxima of the continuous wavelet transform (CWT) along maxima lines to detecting blob. It is related to the largest modulus maximum along some maxima lines of interest. Next, they compute the blob size using the distance between the locations of the modulus maximum of the CWT at the finest scale and the localization of the largest modulus maximum, called maxima line characteristic scale. The proposed method is not based on thresholding technique and can automatic blob detection and blob size determination.

2.3 Exudate detection

Exudates are formed by the leakage of proteins and lipids from the bloodstream into the retina via damaged blood vessels. In retinal images, hard exudates appear as bright yellow lesions with varying sizes, shapes, and locations. Exudate detection technique can apply to developed glistening detection. Thus, exudate detection will be reviewed in this research.

Doaa Youssef et al [16] has proposed fast and an accurate method for early detection of exudates based on detecting areas of higher intensities, yellow color, and high contrast by detecting their contours. The marker image is estimated by dilating the final contours. Then, the full extent of the exudates could be obtained selectively by morphological reconstruction. It could be fully automated after extracting the blood vessel tree, hemorrhage, and optic disc. This algorithm can work properly with lower quality retinal images and images containing hemorrhage and exudates. The proposed algorithm not only detects the blood vessel tree very accurately but also helps in enhancing the detection of exudates using morphological construction methods.

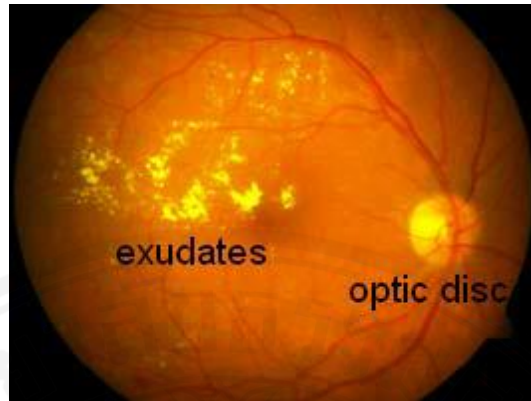


Fig. 2.2 Image with hard exudates [16]

2.4 Drusen

One of the irreversible cause of blindness at the certain stage is Age-Related Macular Degeneration (AMD) [20]. AMD commonly occur in 50 years of age and above and it is leading ocular disease in developed countries [20]. Most of the blindness in Asian countries are based on AMD [20]. It is the third cause of blindness worldwide [21]. Automatic AMD detection and grading are significantly for both clinicians and patients [21].

Drusen is the major sign of early AMD. It is the deposit of waste around macular appearing as yellow-white spots on digital fundus images [21]. Drusen detection is significant important for early AMD detection and drusen segmentation has importance for AMD grading.

Fig. 2.3 shows the comparison of the healthy retina along with retina having hard drusen and soft drusen.

Drusen detection is one of the problems which its technique can apply with our problem. Drusen shown as a bright object in the retina while glistening shown like a bubble or sesame in IOL lens. Thus, drusen detection is reviewed here briefly.

Alauddin B et. al. [22] proposed a novel method to detect drusen. They quantify its size along with the area covered with drusen in the macular region from retinal images. First, they segment drusen from the background using local intensity distribution. Then, applied Gaussian derivative and adaptive thresholding to detect drusen area. The result shows that the 100% accuracy of drusen detection.

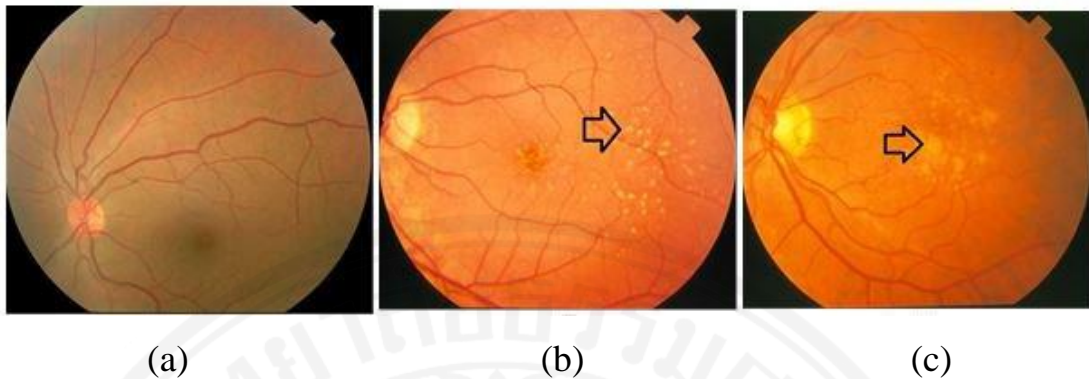


Fig. 2.3 Normal and Abnormal Retinal images a) Normal retinal image b) Retinal image with hard drusens c) Retinal image with soft drusens [20]

M. Usman A. et. al. proposed an automated drusen segmentation for diagnosing age-related macular degeneration. They remove OD pixels along with image enhancement. Then detect the candidate drusen using Gabor filter banks. Finally, SVM classifier is employed to grades the region as drusen or non-drusen. The result shows the system accurately segmented the drusen.

2.5 Watershed Algorithm

Watershed segmentation algorithm based on mathematical morphology is well-known image segmentation approach [23]. Its idea comes from geography which is the gray value of each pixel presents the altitude while every local minimum value and its affecting regions represent basins [24]. This algorithm starts with slowly fill water to the basin. When two or more basins water will be melt, dam, which is a watershed line, will be built between the basins to dividing it. It finishing when all basins already have dam surrounded.

In image processing field, when the dam is built, those pixels is set to 0. In result, all 0 shows as black lines. It's called watershed lines. Watershed lines usually be used for the segmented object from the background or separate two or more object which are touches or closed.

Normally, a watershed algorithm usually leads to over-segmentation because of sensitivity with noise. Marker-controlled watershed segmentation has been presented to be a strong and flexible method for segmentation of objects with closed contours [25] to overcome this problem. It was designed to erase noise by marking region or pixels before normal watershed algorithm processes. By the marker-

controlled technique, the unmarked region will not become to local minimum value, so the number of foreground mark will be the same as the watershed region.

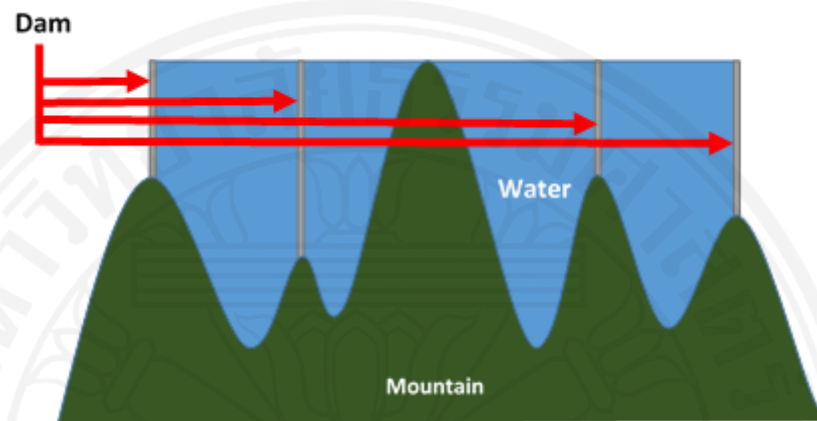


Fig. 2.4 example Image of Watershed algorithm

K. Parviti et. al. [25] have proposed marker-controlled watershed by foreground markers to avoid the over-segmentation problem. They started with creating 'markers image' in the binary image consisting of either single marker points or larger marker regions, where each connected marker's position is inside an object that require segmentation. However, it is difficult to obtain relevant markers automatically without any interaction by the user. They used erosion-based grayscale reconstruction followed by dilation-based grayscale reconstruction to extract the objects while background markers come from calculating the Euclidean distance of binary version of an above-superimposed image. Foreground and background marker is used to modify a gradient image by morphological reconstruction. The result shows that their algorithm is able to segment real image containing severe irregularities.

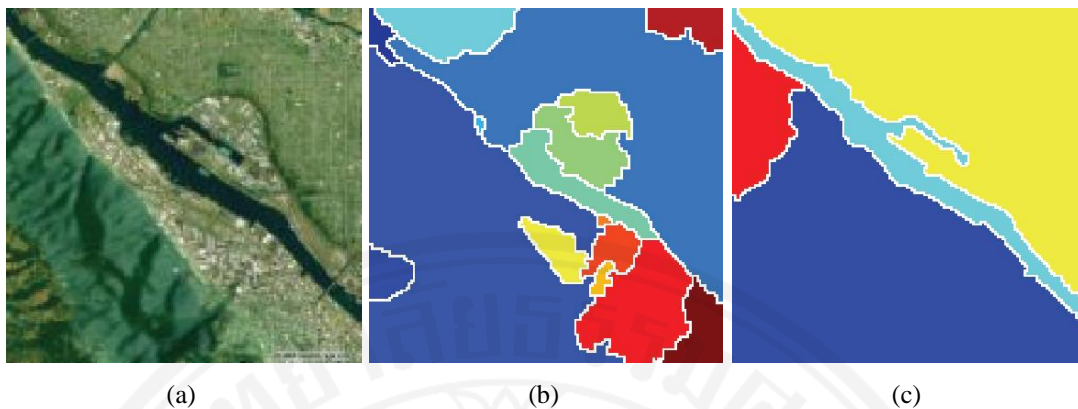


Fig. 2.5 Image of Marker-Controlled Watershed algorithm result. a: Original image, b: Result of original watershed algorithm, c: Result of Marker-Controlled Watershed algorithm [25]

Chapter 3

Automatic blob-based glistening detection in intraocular lens

3.1 Introduction

Glistenings can affect human vision by increasing forward light scatter [7–9]. An effect is varying by a difference of size, density and location of glistenings [10]. A few studies suggest other groups look for the glistening detection using image processing technique. We apply blob detection and exudate detection to design glistening detection. Blob corresponds to circular like regions that are either brighter or darker than their surroundings or in the same color in the image or video [12], [13]. Basically, the blob can be detected by thresholding the image, or its bounds can be defined by edge filter [14]. The leakage of proteins and lipid from the bloodstream into the retina via damaged blood vessels, called exudate [15], [16]. Hard exudates are shown as bright yellow lesions with varying sizes, shapes, and locations in the retinal image [16]. It appears like blobs in the retina.

3.2 Software for the Quantification of Glistenings in Intra-Ocular Lenses

Software for the Quantification of Glistenings in Intra-Ocular Lenses is designed by Parisut J.[10]. This software is a collaboration between researchers from Thammasat University in Thailand, Kingston University and City University in London. It is designed to be user-friendly and semi-automatic for glistenings detection so inexperienced users supply simple information to get the best-detected result. Those informations which are required for detecting glistenings, consists of input IOL image for glistening detection, lens mask size, maximum area of glistenings, minimum area of glistening, maximum threshold value, minimum threshold value and step of a threshold value.

Fig. 3.1 shows the glistening quantification software image. The software has 8 features for glistenings quantification including image selection and display, lens detection, parameter configuration and glistenings detection, ground truth selection, layer selection, quantification result and validation details.

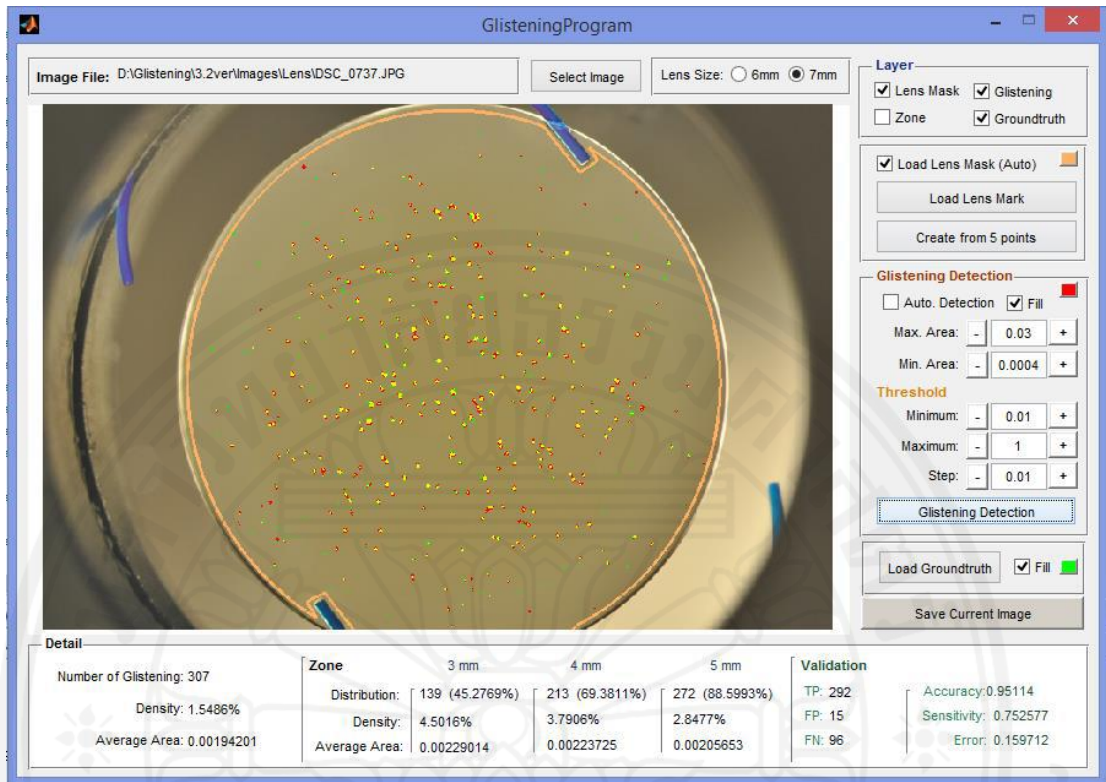


Fig. 3.1 Screen of software shows the comparison of detected glistenings and the ground truth.

a) IOL Image Selection and display

This feature, user can select the IOL input image by opening the image file from 'Select Image' button. The IOL image can be 4 types: JPG, TIFF, PNG, or GIF.

b) Lens Detection

Before the glistenings detection algorithm can be processes, the software needs to specify the region of the lens. This software consists 2 ways to identify the boundary of the lens. First, the user can load the lens mask by selecting the lens mask image file where the white area is the region of interest of the lens. If the user doesn't have a mask, the user can create a mask semi-automatically by specifying 5 different locations on the lens boundary. The lens mask area is then created by the program and shown on the screen.

c) Glistening Detection

In the glistenings detection feature of the software, the user can adjust various parameters for a variety of glistenings image input. There are 5 variables in this part consisting of Maximum area of glistenings, Minimum area of glistenings, Minimum Thresholding value, Maximum Threshold value and step of thresholding value. The user can choose the color of the glistenings and choose to show only the boundary line or the glistenings area filled with color.

d) Ground truth Selection (for development phase)

After the program validation phase, the user can load a ground truth image and compare it with the automatic glistening detection result. Accuracy and Sensitivity will be automatically calculated.

e) Layer Selection

The user can select the layers to be shown on the IOL image. There are 4 layers in the software; Lens Mask, Zone, Glistenings, and Ground truth.

f) Image Saving

A Save current image button is also added to help the user save the current processed image easily.

g) Quantification results

The results of the glistenings detection algorithm is shown on the Quantification Detail. The Overall result is shown on the bottom of the screen for easy access. The results consist of the number of glistenings, density and average area. The next panel shows results from each zone of the IOL lens which can represent the pupil of human eye. The results show the distribution, density and average area of each zone.

h) Validation Result

The accuracy and sensitivity are used to compute frontend performance. The accuracy is the result of the correct result divided by the total number of

classifications and sensitivity is the result of the true positive and the condition negative. After the user choses a ground truth image, the true positive (TP), false positive (FP), false negative (FN), accuracy, sensitivity and error are be shown on the right hand side of the detail section.

3.3 Glistening Detection Algorithm

The glistening detection algorithm is developed from Blob detection and exudate detection because glistening appears like a blob in IOL lens. There are 6 big steps in glistening detection algorithm, namely pre-processing, edge detection, connecting broken lines and filling holes, boundary hardening, candidate classification, and finally candidate selection. Flow chart of glistening detection technique is shown in Fig 3.2.

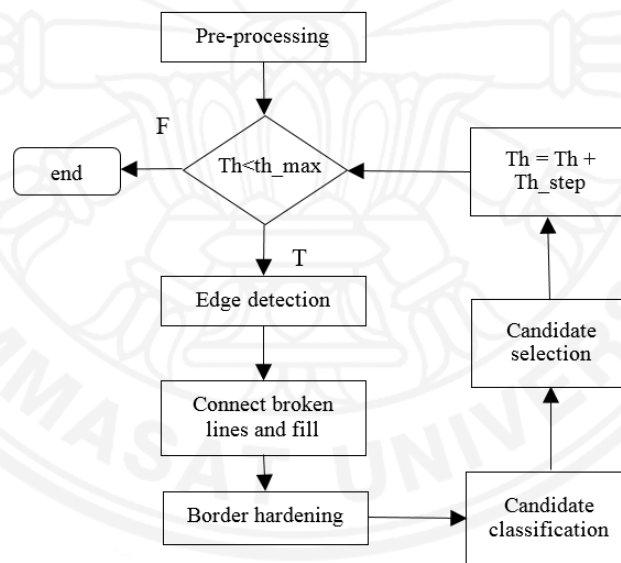


Fig. 3.2 show flow chart of glistening detection method

a) Pre-processing

Pre-processing steps consists of 2 parts. First the size of the images are normalised and resized to 750 pixels in width to reduce the difference in image size and resolution.

With the prior experimental results, we found that glistenings have a good response in a Red channel for the RGB color model. The red channel is then extracted and used as the next step's input.

Fig 3.3-3.5 indicate the difference of original image, red channel extraction image, green channel extraction image and blue channel extraction image while, Fig. 3.3-3.5 (a) are original images. Fig. 3.3-3.5 (b) are red channel images. Fig. 3.3-3.5 (c) are green channel images and Fig. 3.3-3.5 (d) are blue channel image.

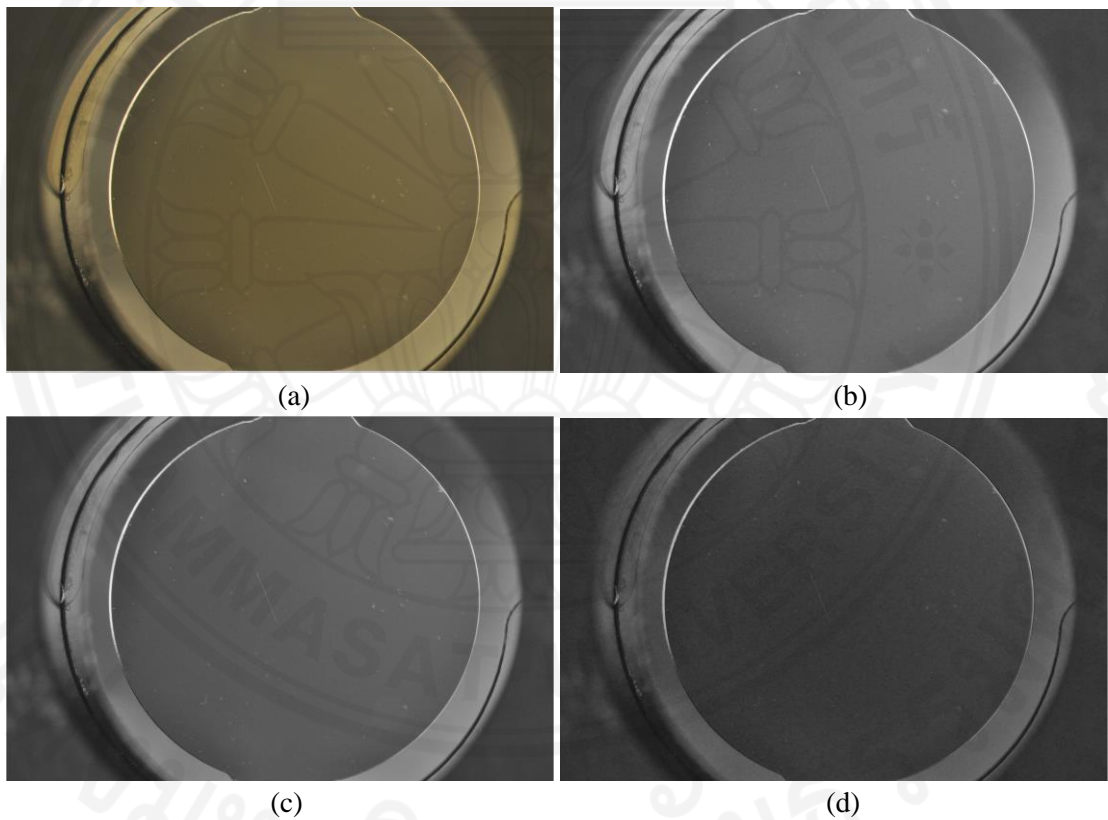


Fig. 3.3 Comparison of Original image and Red, Green, Blue channel extraction
(set 1)

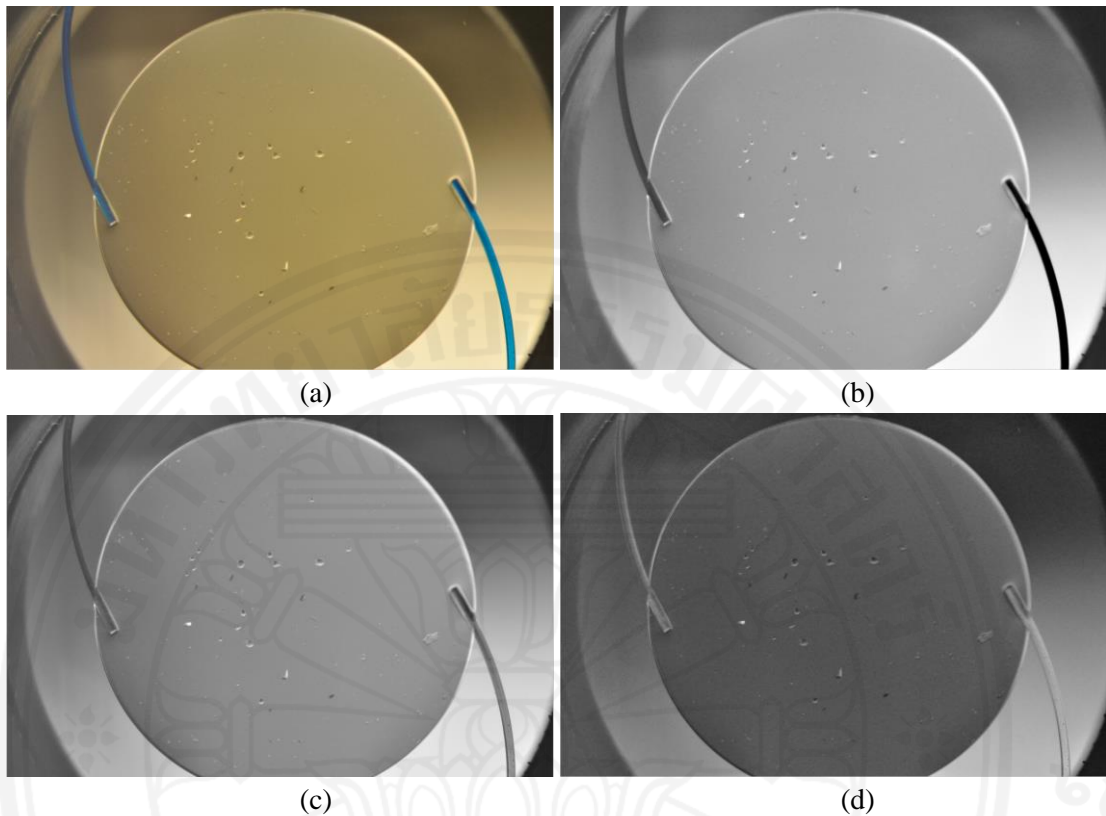


Fig. 3.4 Comparison of Original image and Red, Green, Blue channel extraction
(set 2)

b) Edge detection

Most of glistening have no color (transparent) in IOL image. Thus, the edge will be a good representation of the glistenings because of the shadow of glistening. In order to find the edge, we applied both vertical Sobel and horizontal Sobel filters to the image. The results of each pixel are the number of gray level from 0 to 1 in each pixel. In this step, the threshold value which user set in Glistening software is used to remove the noise. The first threshold value is set to the minimum threshold value. Then, in case of result of Sobel operation is less than threshold value, the value in this pixel is set to 0 but if result of Sobel operation is more than threshold value, the value in this pixel is set to 1. In the end, the result of both directions is combined by or operation.

Fig. 3.6 and 3.7 show results of the Sobel filter with 0.02 threshold value and Fig 3.8 and 3.9 show results of Sobel filter with difference threshold value.

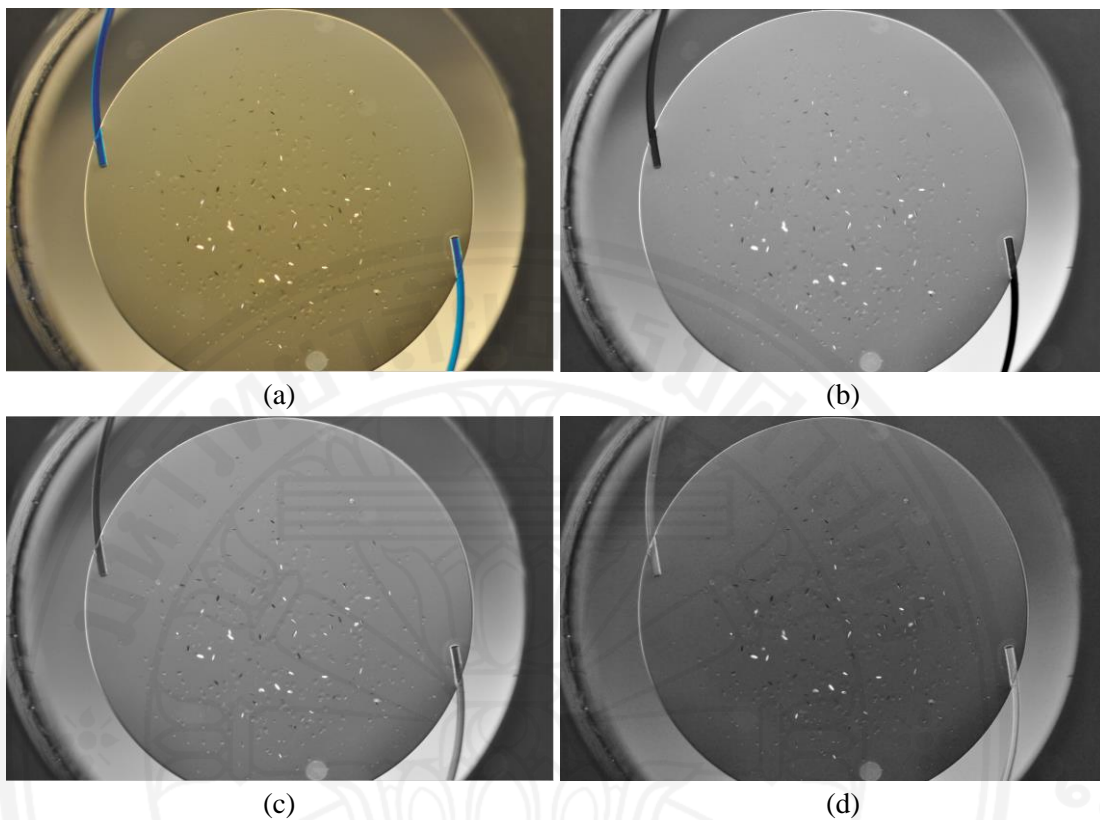


Fig. 3.5 Comparison of Original image and Red, Green, Blue channel extraction (set 3)

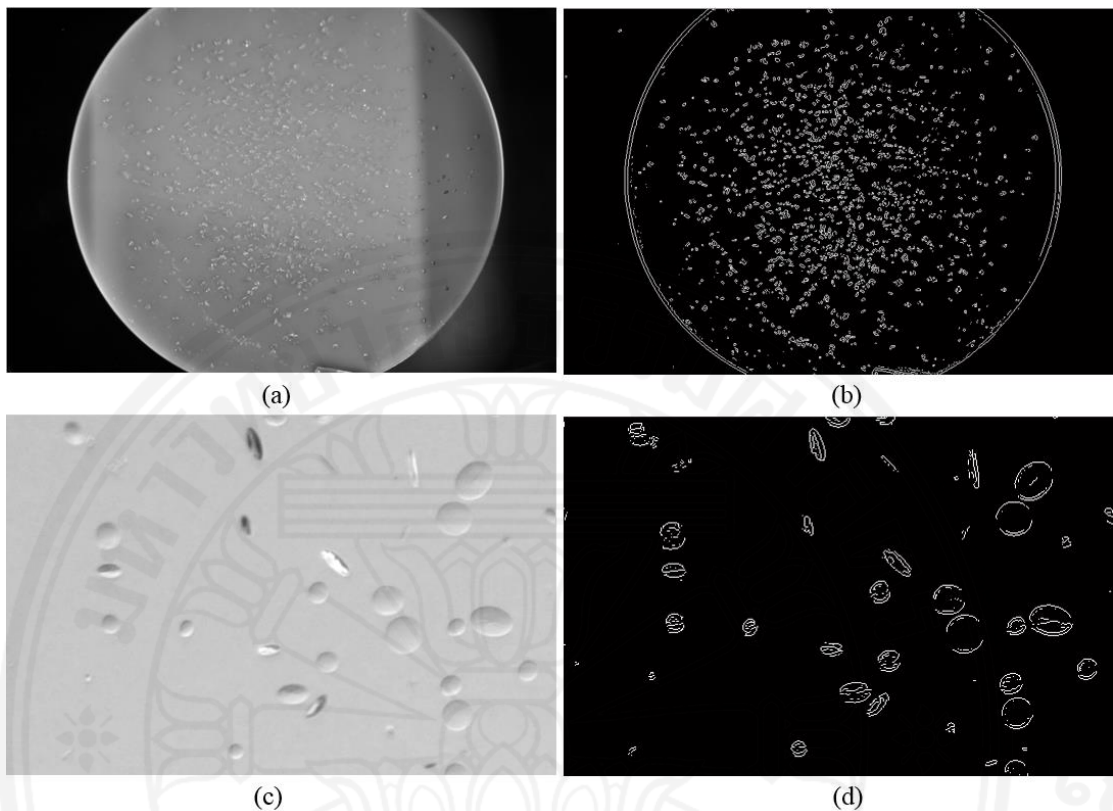


Fig. 3.6 Edge detection result (a) and (c) IOL image before Edge detection (b) and (d) IOL image after Edge detection threshold value equal to 0.02 (set 1)

In addition, because of IOL image includes IOL area and non IOL area (the area outside the IOL lens). Lens mask data is used in this step to erase noise outside the IOL. Lens mask data can be get by the user in Glistening program which explained in 3.2 b). All edges which are detected out size Lens mask area would be set into 1. Thus, all area out size IOL lens would be black.

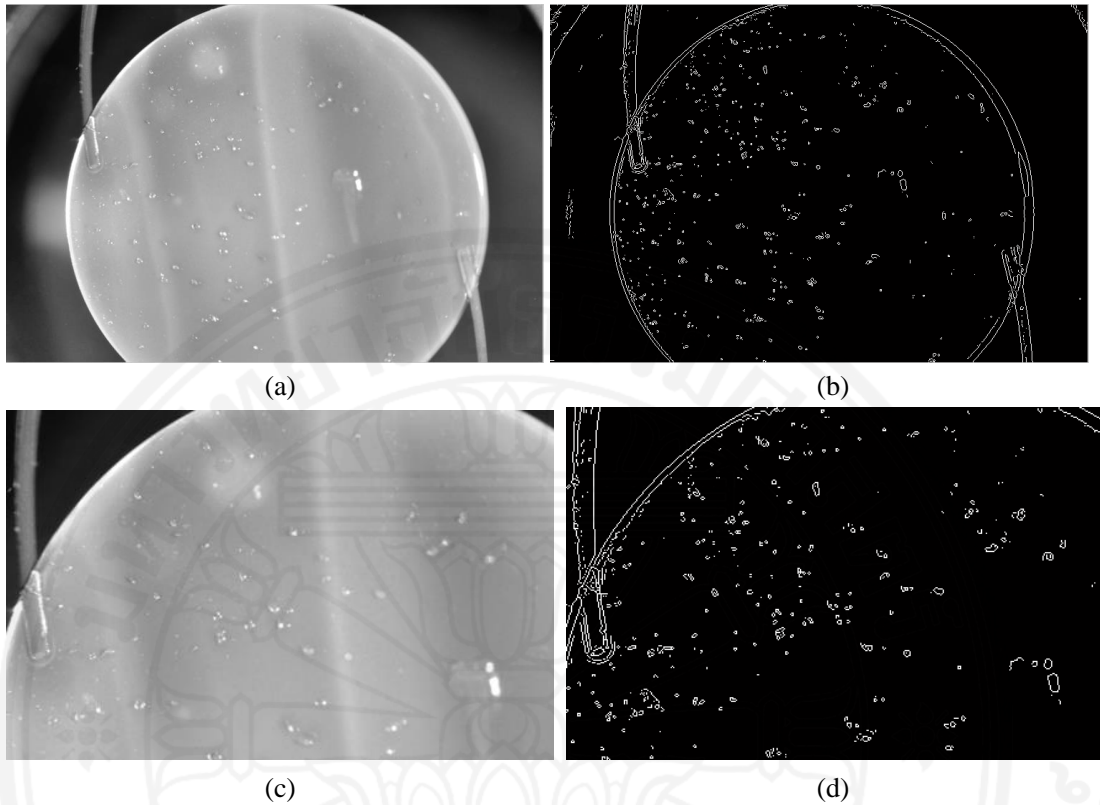


Fig. 3.7 Edge detection result (a) and (c) IOL image before Edge detection (b) and (d) IOL image after Edge detection threshold value equal to 0.02 (set 2)

c) Connect broken lines and fill holes

Lines from Sobel filter tend to be broken due to the result of edge detection varies according to the quality of the original image. Thus, Dilation Operation is applied to overcome this problem with mask in Fig. 3.10. The dilation operation is the basis operation of mathematical morphology to analyze and process geometrical structure of images. Dilation operation provides thicken and lengthen edge of glistening. Therefore, broken lines can be connected by dilation operation.

After the line connection process, we fill the glistening with foreground color using the hole-filling technique all background color pixels which are confined by borders would be changed into the foreground. So, the area of glistening is defined. The example results from each step of this process are shown in Fig. 3.11 and 3.12.

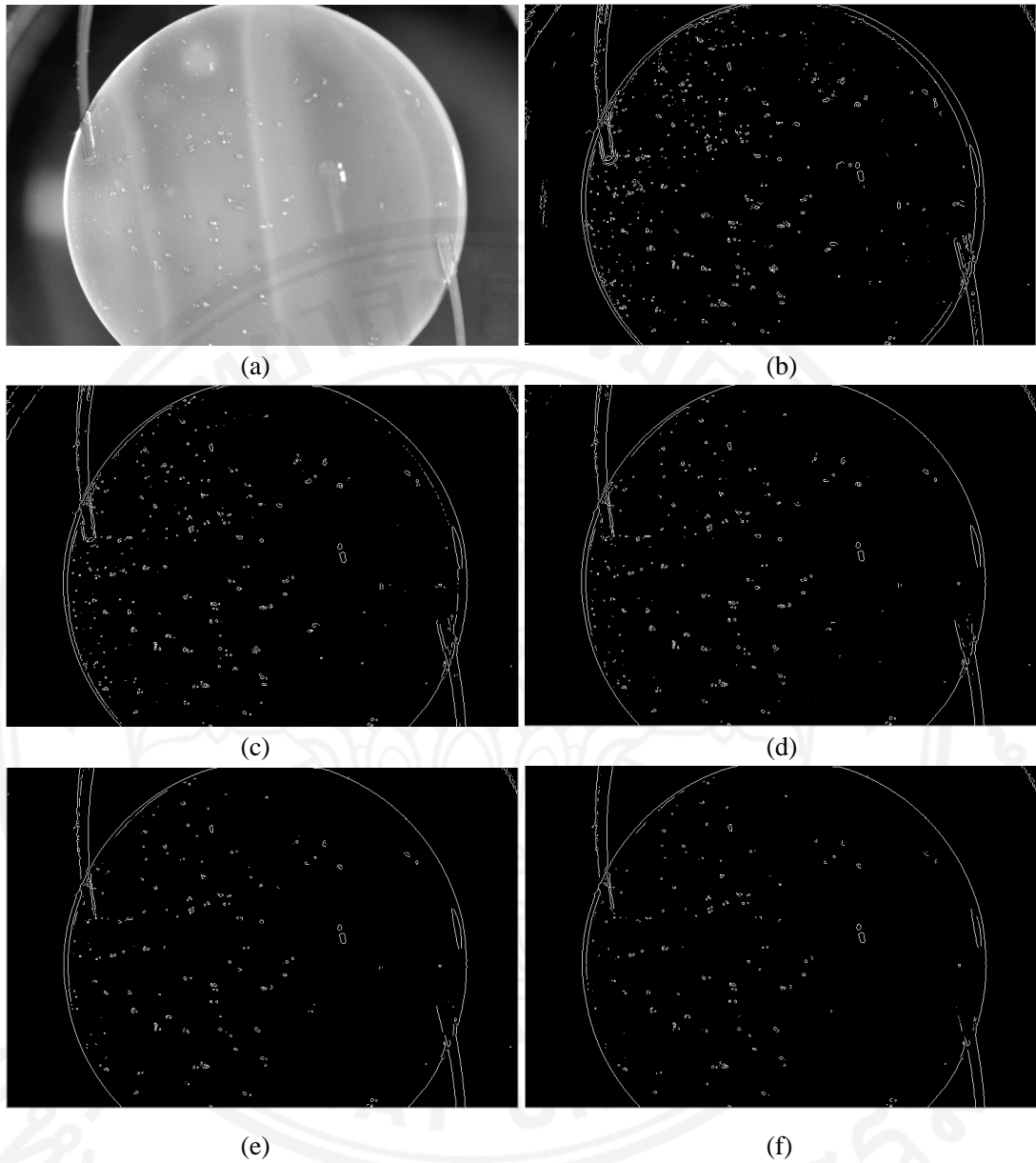


Fig. 3.8 Sobel operation result with difference threshold value (a) red channel extract from input image, (b) result image with threshold value = 0.01, (c) result image with threshold value = 0.02, (d) result image with threshold value = 0.03, (e) result image with threshold value = 0.04, (f) result image with threshold value = 0.05 (set 1)

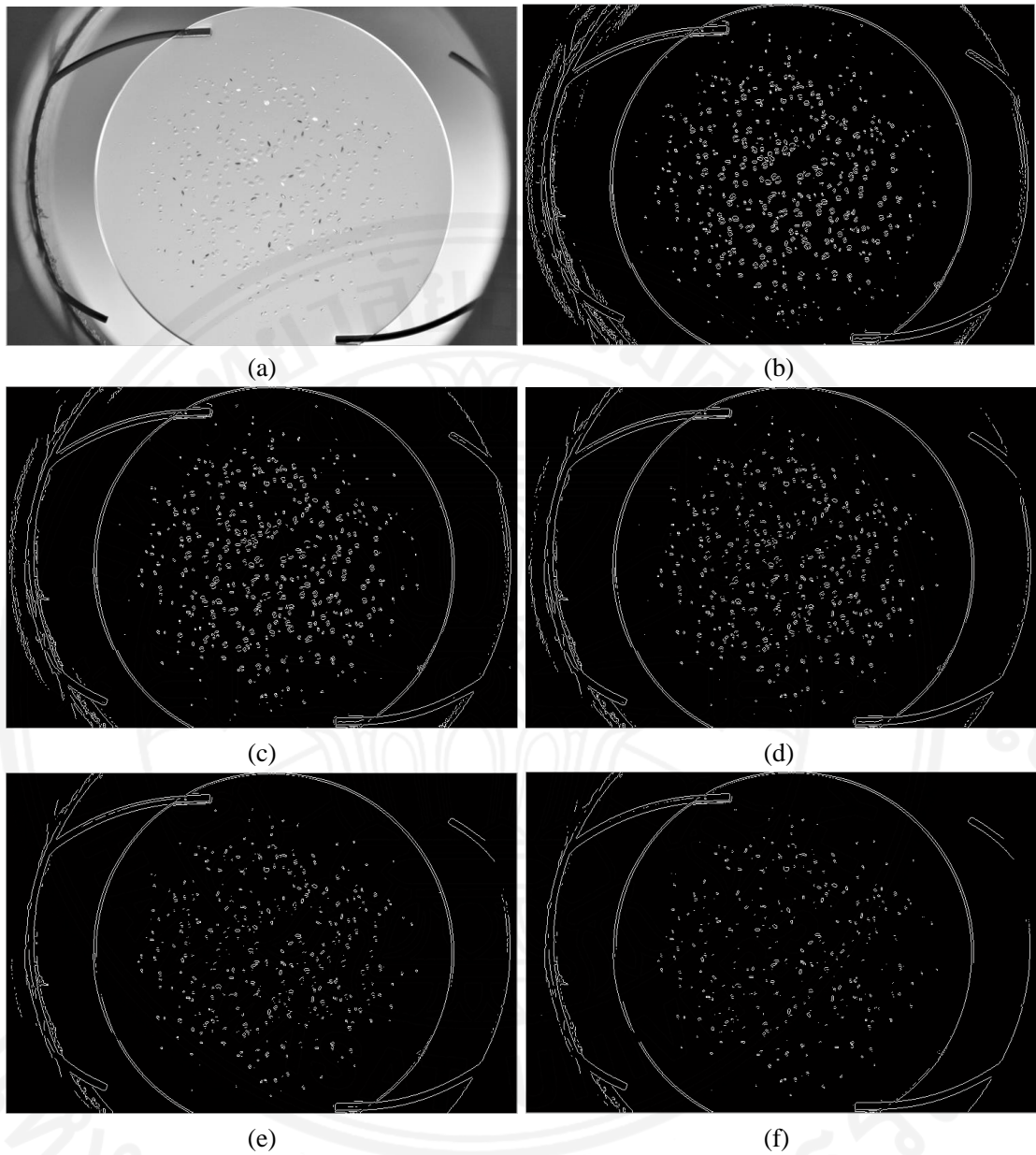


Fig. 3.9 Sobel operation result with difference threshold value (a) red channel extract from input image,(b) result image with threshold value = 0.01, (c) result image with threshold value = 0.02, (d) result image with threshold value = 0.03, (e) result image with threshold value = 0.04, (f) result image with threshold value = 0.05 (set 2)

0	1	0
1	1	1
0	1	0

Fig. 3.10 Mask for dilation and erosion operation



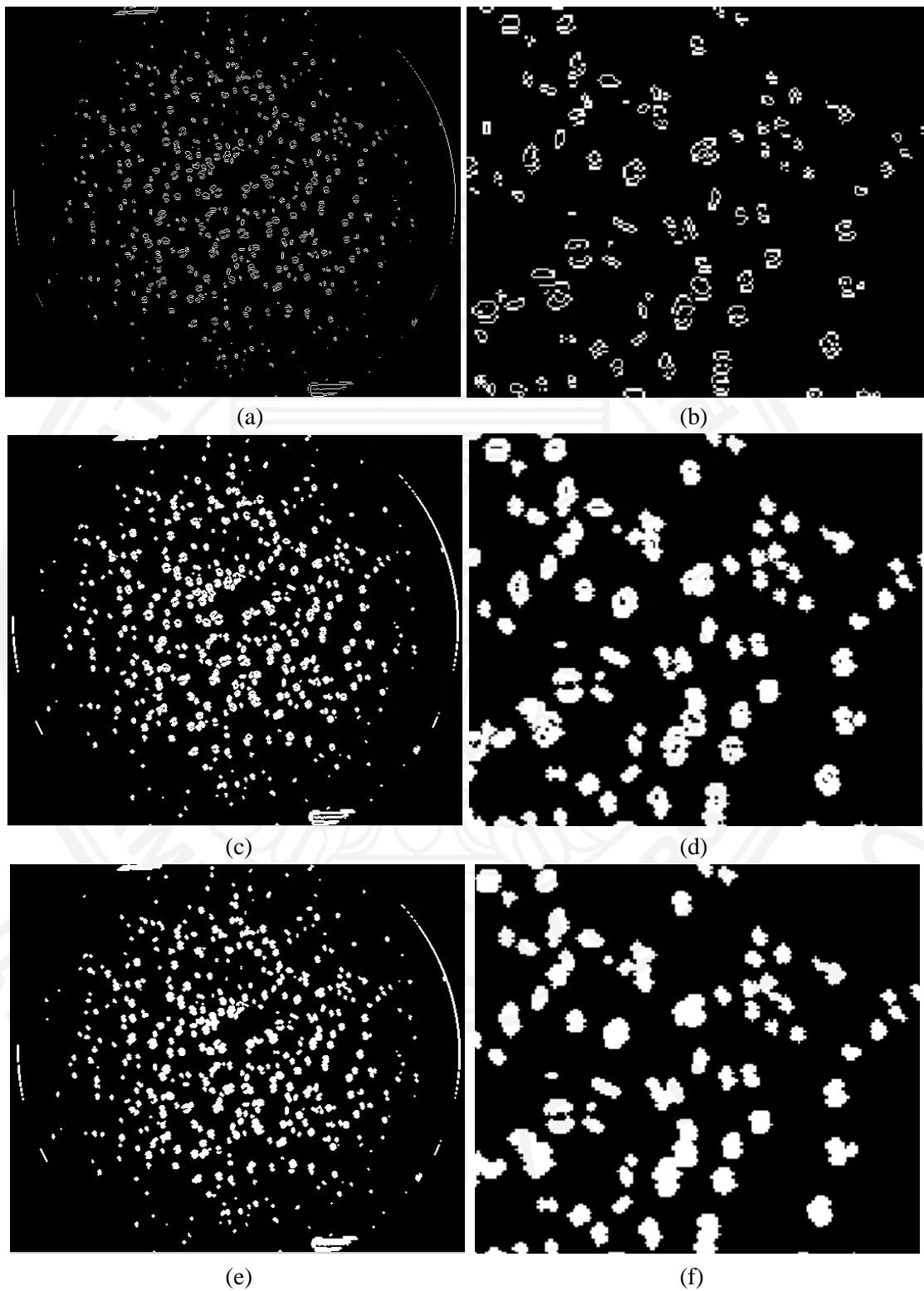


Fig. 3.11 Example of connect broken line and fill holes step (a) and (b) result from edge detection step, (c) and (d) result of 1st dilation operation, (e) and (f) result of fill holes process (set 1)

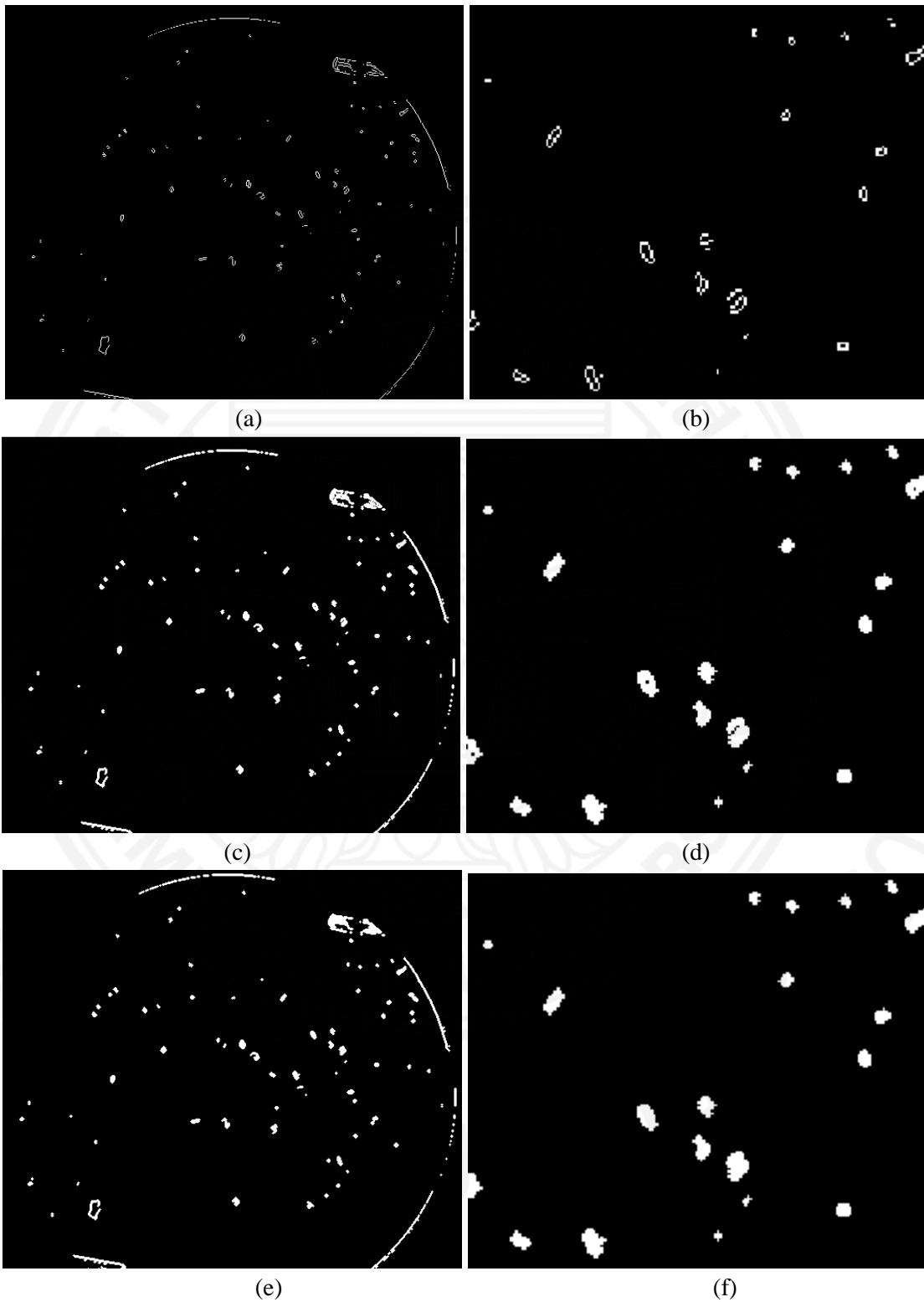


Fig. 3.12 Example of connect broken line and fill holes step (a) and (b) result from edge detection step, (c) and (d) result of 1st dilation operation, (e) and (f) result of fill holes process (set 2)

d) Border hardening

We have candidate regions for glistenings after the previous step. However, many of edge boundaries are still irregular. We then repeatedly use dilation operation for one time to straighten the boundary. However, dilation operation makes the area of detected glistening larger than the real size. Therefore, we applied erosion operation twice to smoothen the boundary and change the size of detected glistening. Erosion operation also the mathematical morphology which can analyze and process geometrical structure of images. While dilation operation makes line thicken and lengthen, erosion operation provides thinner and shorter lines. Due to, the previous step we apply twice of dilation operation. So, we use erosion operation twice too and the mask for erosion operation is the same mask of dilation operation shown in Fig. 3.10. The result of smoother blobs from this step is shown in Fig. 3.13 and 3.14.

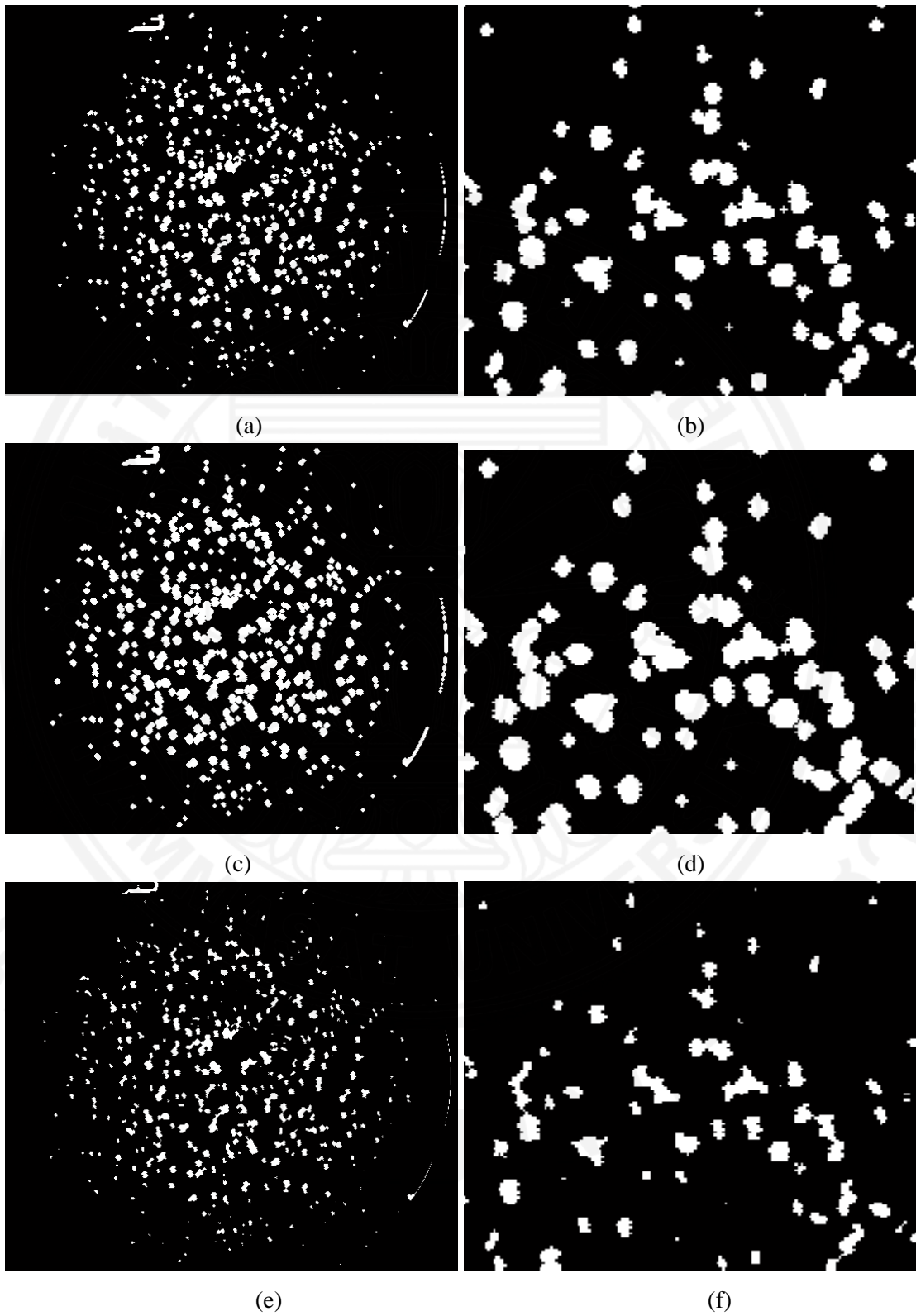


Fig. 3.13 Example of border hardening step (a) and (b) input from original image, (c) and (d) dilation filter result, (e) and (f) twice erosion filter result (set 1)

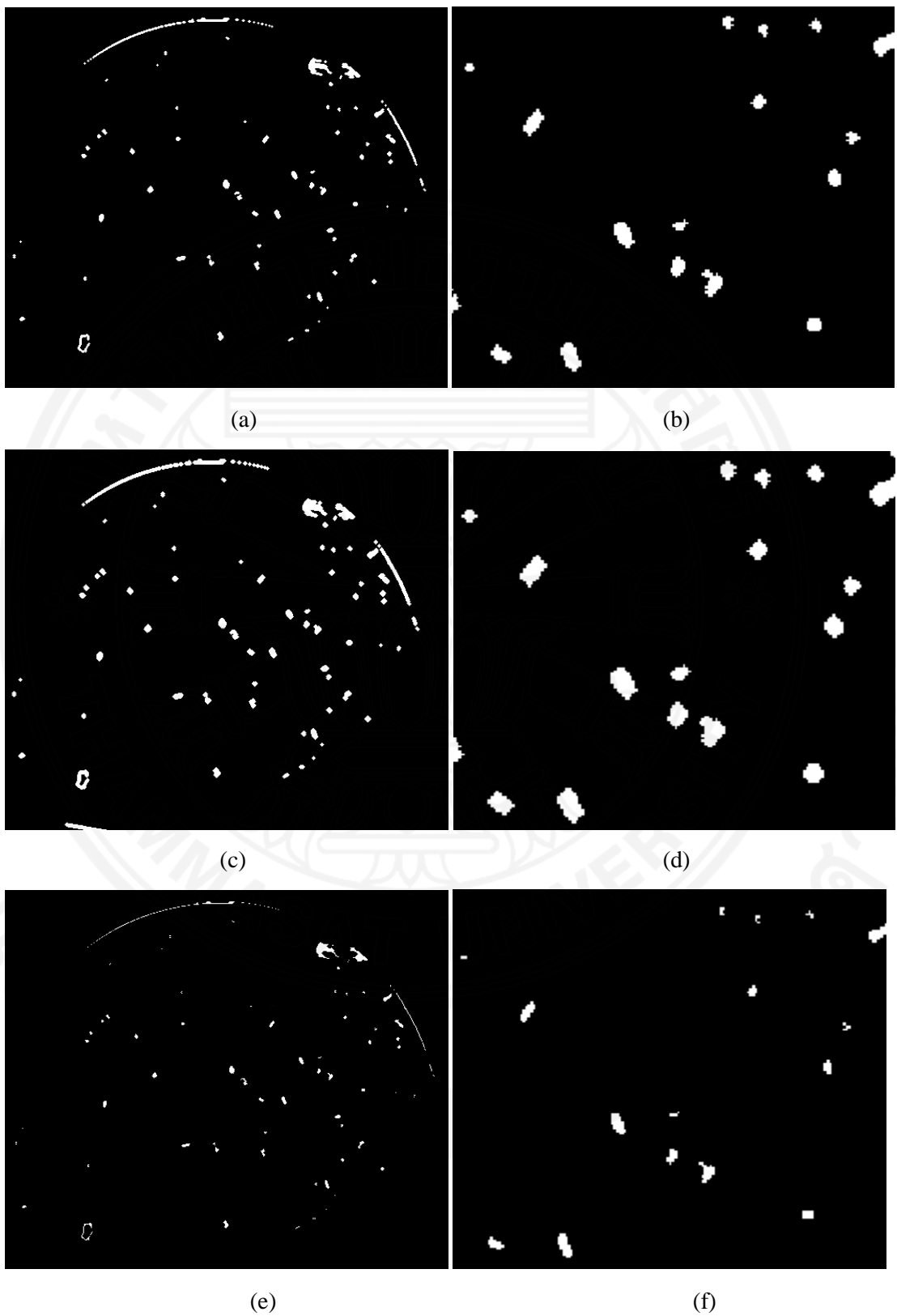


Fig. 3.14 Example of border hardening step (a) and (b) input from original image, (c) and (d) dilation filter result, (e) and (f) twice erosion filter result (set 2)

e) Candidate classification

Sobel operation has a high performance for edge detection. However, it also provides a sensitivity of noise. IOL image always consists of noise and sometimes the boundary of the handle of IOL is detected. In this step, we removed the false candidates using the size thresholds specified by the user. Meaning that the blobs size that are too big or too small will be removed from the candidate blob list. The result of candidate classification step shown in Fig. 15. If user put the appropriate value for minimum area of glistening and maximum area of glistening, all noise would be erased.



Fig. 3.15 Candidate classification result, (a) input image, (b) result

f) Candidate selection

Because we have many potential candidates to be classified as glistening, the result from the previous step has to be thresholded. Nevertheless, glistenings have different sizes and shapes. They are also different in terms of clarity. So, one threshold doesn't fit all. We varied the threshold from step B to E. With each step we have different thresholded results. The thresholded start from the minimum threshold value to the maximum threshold value whereas the step is the threshold step. All 3 values are specified by the user to get the good result for each IOL image. Results of every threshold value will then be combined using OR operation and that will become our final results. Fig. 3.16 and 3.17 show the result of candidate classification with difference thresholded and the final result. Fig 3.18 presents the result of final results of various IOL images with different input data.

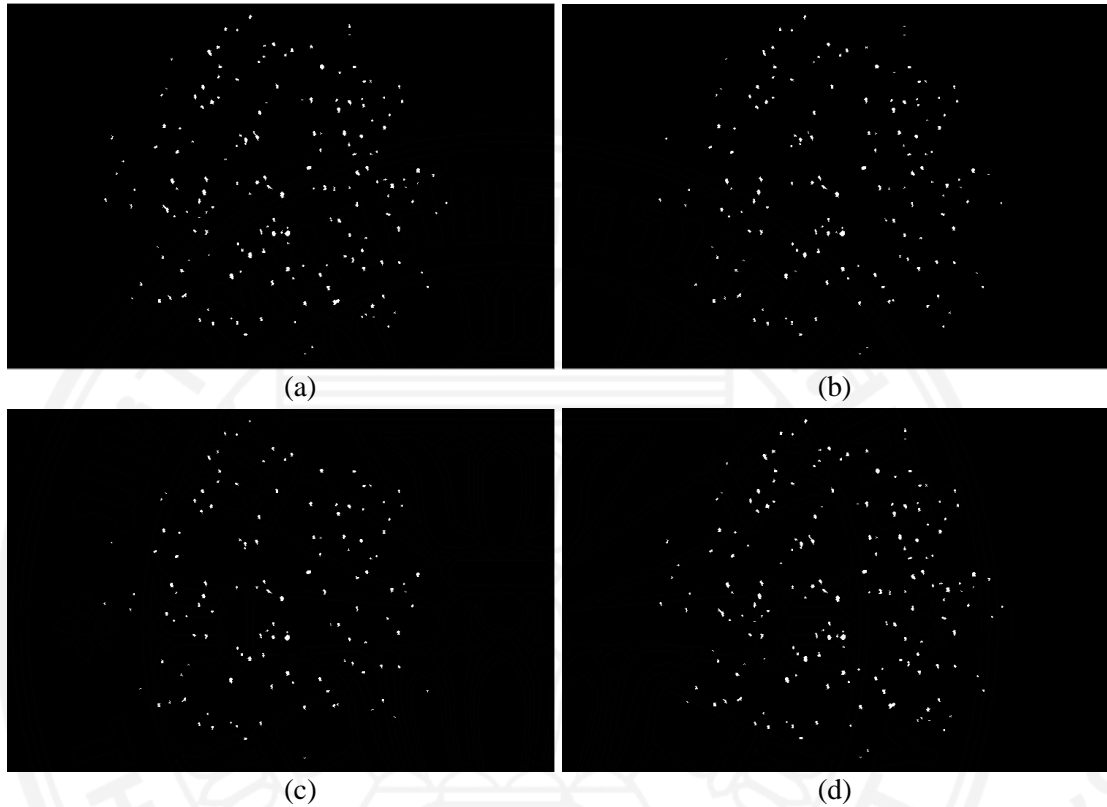


Fig. 3.16 Candidate classification result in different threshold value, (a) Threshold value = 0.03, (b) Threshold value = 0.04, (c) Threshold value = 0.05, (d) Final Result from (a), (b), (c) with OR operation (set 1)

3.4 Conclusion

The software for quantification of Glistening in Intra-Ocular lens is presented in this chapter. Its features are shown for the overall process of this software. Then, Glistening detection Algorithm is carefully explained. Blob-based detection algorithm is applied in glistening detection process. The result image of each step is also presented for more understanding.

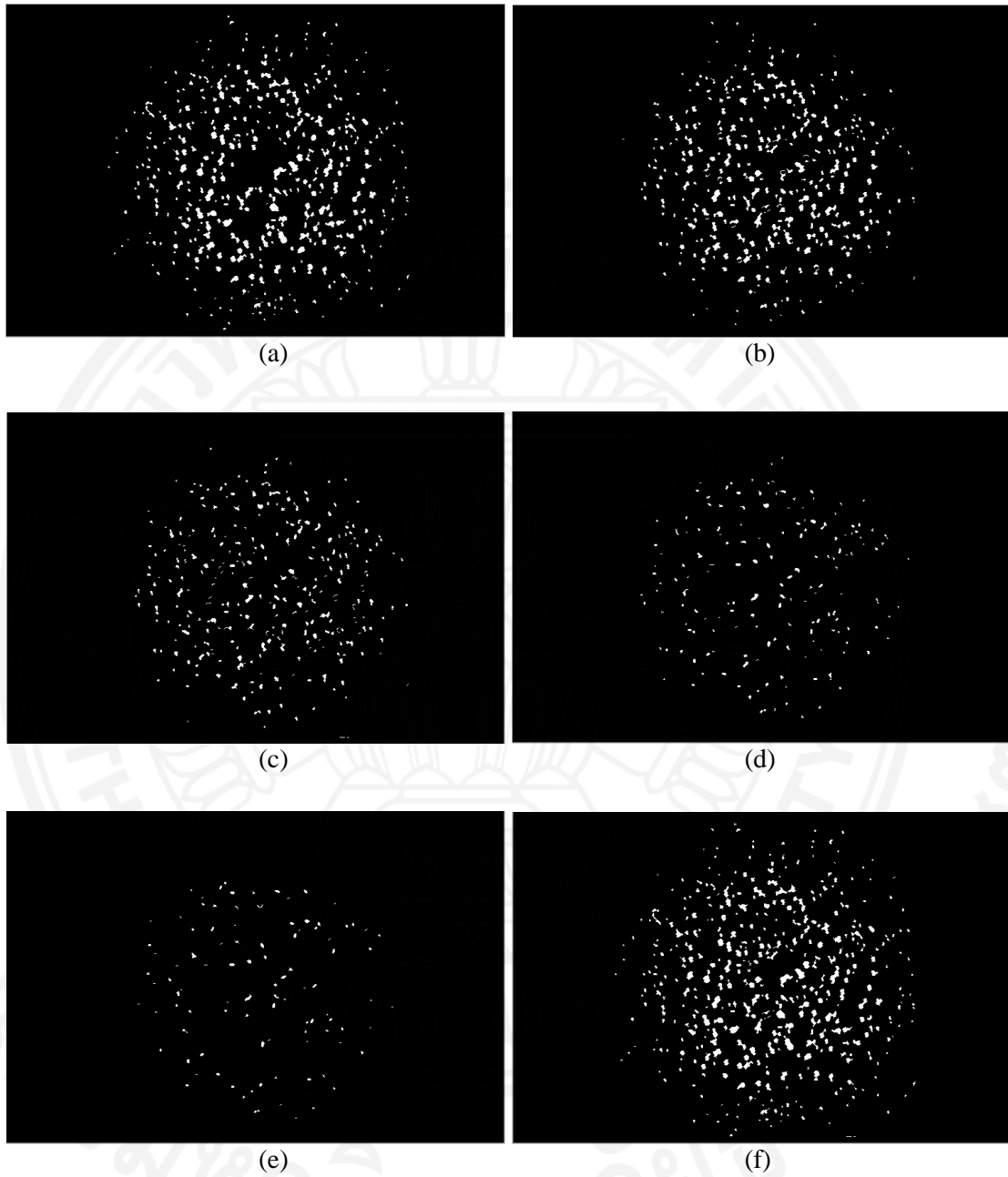
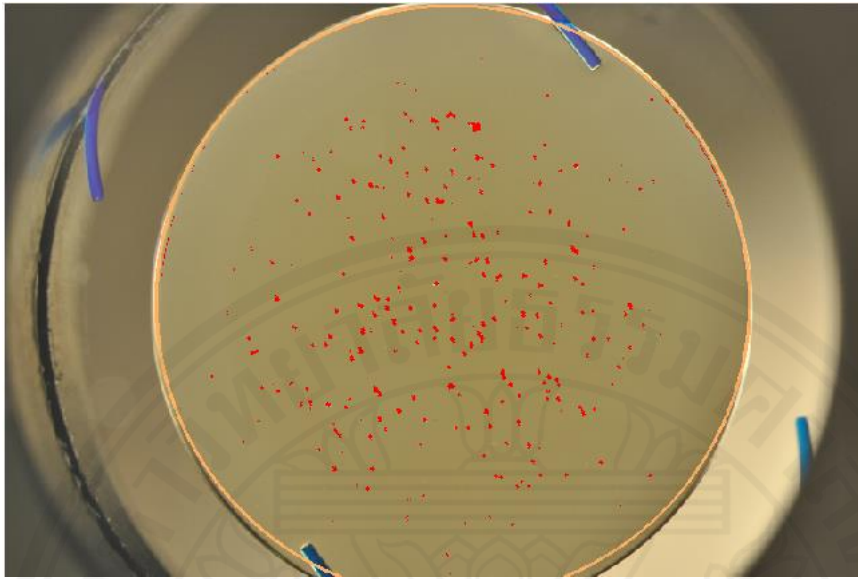
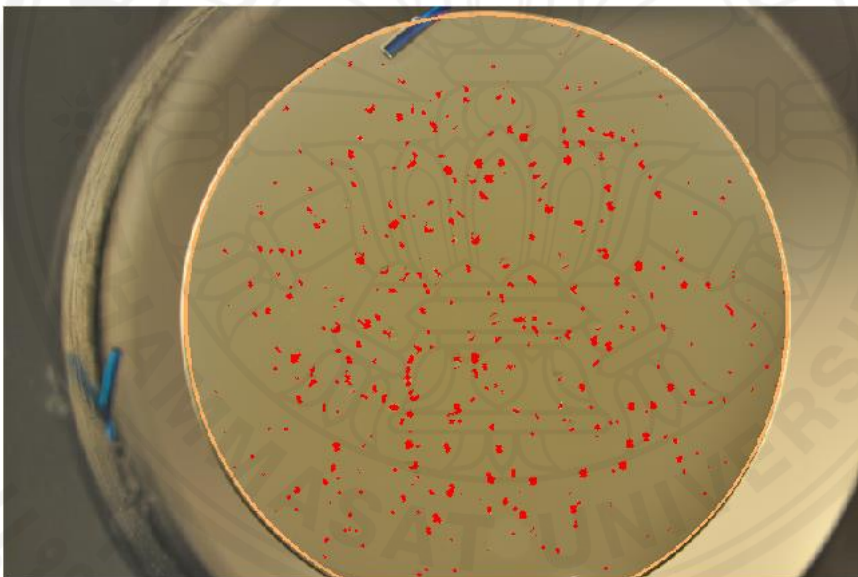


Fig. 3.17 Candidate classification result in different threshold value, (a) Threshold value = 0.01, (b) Threshold value = 0.03, (c) Threshold value = 0.05, (d) Threshold value = 0.07, (e) Threshold value = 0.09, (f) Final Result from (a), (b), (c), (d), (e) with OR operation (set 2)



Glistening area
Max: 0.03
Min: 0.0001
Threshold
Max: 1
Min: 0.01
Step: 0.02



Glistening area
Max: 0.01
Min: 0.0001
Threshold
Max: 1
Min: 0.01
Step: 0.01

Fig. 3.18 Glistening algorithm result

Chapter 4

Quantification of the overlapped glistening in intraocular lens

4.1 Introduction

The previous chapter we proposed an algorithm for accuracy detect glistening. It was designed to semi-automatically detects glistening. However, this algorithm still has a limitation with computing the number of glistening. Overlapped, touch and closed Glistenings were defined in one region, so, the number of glistenings were counted only one glistening instead of the actual number. Image segmentation is a basic issue in the field of image processing [26, 27]. Its role is to segmenting the image into the different feature of region [26] or dividing an image into distinct regions, mainly corresponding to interested objects in a background [23]. The watershed algorithm, based on the morphological principles, is a well-known image segmentation approach [23]. It segments an image by find dividing lines [28]. These dividing lines are work like watershed which outlines each outer catchment basins which are the local minimum value within image [28]. The watershed approach certifies boundaries on the image plane to be connected and closed, and each gradient at least corresponds to one area [29]. However, it exists some drawback because of noise sensitivity, it yield over-segmentation as each local minimum will form a catchment basin [23, 29, 30, 31]. Many methods are proposed to solve over-segmentation problem such as marker image [23], gradient transformation, multi-scale gradient and distance transformation [28], anisotropic filter [23], adaptive threshold [31], and marker-controlled watershed [25].

However, various kind of watershed technique cannot use in glistening detection technique because normally in image one glistening consists of 2 parts which are light region and dark region because of it curve reflex the light. According to the capability of watershed technique, in this chapter, we applied the watershed algorithm to calculate skeleton by influence zones to separate glistenings. It can automatic separate overlapped, closed and touched glistening after glistening detection algorithm is processed. The proposed method can increase performance of glistening detection technique in numerical field.

4.2 Glistening separation process

Glistening separation process applies the watershed technique to separate closed, touched, and overlapped glistening. The overall process was given in Fig. 4.1. It mainly composes of 4 steps, including pre-processing, foreground extraction, watershed algorithm and combine result. Original glistening detection result is used in the last step to revise result. Separated glistening result of proposed technique is binary image as same as glistening detection result.

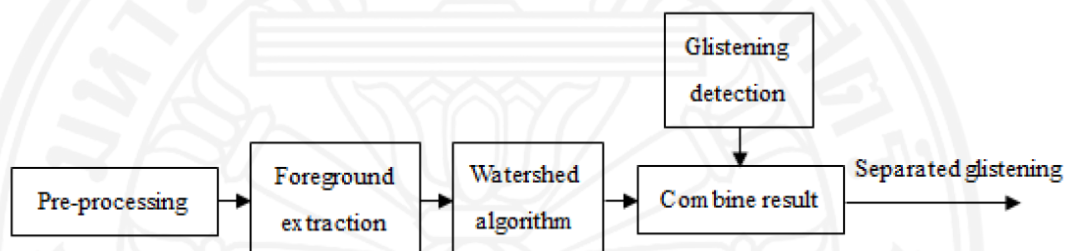


Fig. 4.1 Glistening separation flowchart

a) *Pre-processing*

In pre-processing process, the IOL input image is changed from RGB color space into the grayscale image for preparing image because the watershed algorithm works with the grayscale image. Background of IOL image always has difference color because of the light. To make a high-performance algorithm, we resized all image to 750 pixels of width and divided it into several small images to get difference gray level of each zone. So, IOL image is divided into 25 images. Size of it is the same.

b) *Foreground extraction*

Foreground marking is the step to marker object region for computing skeleton of glistening. Otsu thresholding technique is employed in this step. Basically, glistening within IOL image shows both darker region which are shadow of glistening and brighter region which reflected the light. Otsu thresholding technique can detect darker region or brighter region in IOL image. It depends on the intensity of gray

value of the background image. However, extracted area should be white. So, after Otsu glistening method is processed, the proposed method checks which region is detected. If detected region is the darker region, all pixels are converted, 0 pixel changes to 1 and 1 pixel changes to 0. Fig.3.11 (a) and (c) are original IOL images. Fig.4 (b) and (d) shows the result when Otsu method detected darker region and brighter region, respectively.

To check which region was detected, first we calculated the number of white regions. If there is a white region then, we compute the major-axis and minor axis of a white area in the thresholded image and the major axis and minor axis of the original image. For example, Fig. 4.2 (d), the number of the white region is one. Thus, the size of major-axis and minor axis are calculated then comparing with Fig. 4.2 (a). If the both area are similar, ± 5 pixels, the image is converted.

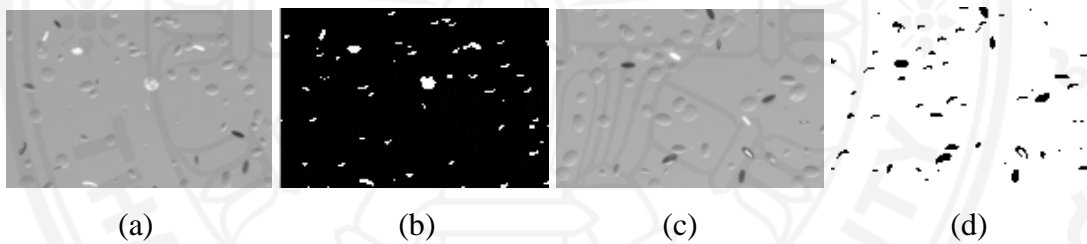


Fig. 4.2 Example when Otsu thresholding method difference detected.

c) *Watershed Algorithm*

Watershed segmentation algorithm based on mathematical morphology is well-known image segmentation approach [23]. Its idea comes from geography which is the gray value of each pixel presents the altitude while every local minimum value and its affecting regions represent basins [24]. This algorithm starts with slowly fill water to the basin. When two or more basins water will be melt, dam, which is the watershed line, will be built between the basins to dividing it. It finishing when all basins already have dam surrounded.

Normally, the watershed algorithm usually leads to over-segmentation because of sensitivity with noise. Marker-controlled watershed segmentation has been presented to be a strong and flexible method for segmentation of objects with closed contours [25] to overcome this problem. It was designed to erase noise by marking

region or pixels before normal watershed algorithm processes. By the marker-controlled technique, the unmarked region will not become to local minimum value, so the number of foreground mark will be the same as the watershed region. However, marker-controlled watershed still followed over-segmentation with glistening.

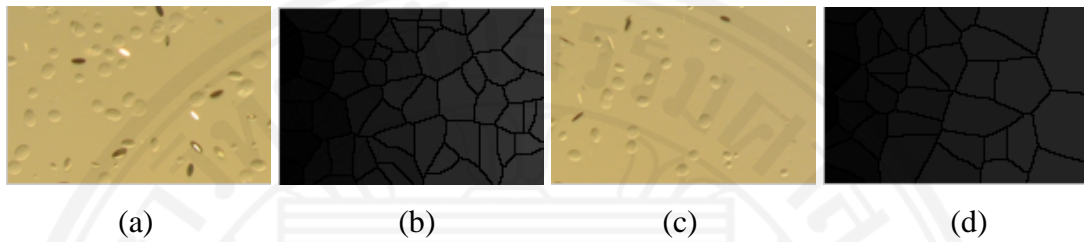


Fig. 4.3 Example of watershed result of IOL image.

Thus, instead of using the watershed algorithm to separate glistening, the watershed algorithm is used for computing skeleton by influence zones of glistening to avoid over-segmentation. The watershed algorithm is employed with the result in the previous step. The result of watershed ridge lines represents the border of glistening.

Fig. 4.3 (b) and (d) shows the example of watershed ridge line and fig. 5 (a) and (c) are original IOL images.

d) Combine result

Combine result process works with 2 results, glistening detection algorithm from the previous chapter and watershed algorithm process. From glistening detection process, we can get the glistening region. All white areas are detected glistenings and black region is background as shown in fig.1 (b). Watershed ridge lines are black lines. Thus, Eq. 1 is operation between glistening detection image result and watershed algorithm result. Whereas, GD is the glistening detection result and WT is the watershed algorithm result. So, using eq. 1, we can use lines from watershed algorithm process to dividing both overlapped glistening and touch glistening.

$$\text{Separated glistening} = WT \wedge GD \quad (1)$$

Fig. 4.4-4.6 show the final results of glistening separation algorithm. Fig. 4.4 and 4.5 present the good result of glistening separation although sometimes the IOL image is hard to detect by human eyes.

Fig 4.6 presents some problems which still show in the proposed method. Fig 4.6 row 2 and 3 shows the over-segmentation result. Row 1 is the problem from glistening detection which cannot detect glistening perfectly. It provides over-segmentation although this proposed method is work-well. Row 3 is the result when the proposed method cannot work.

4.3 Conclusion

To increase performance of the glistening detection method, glistening separation process is presented in this chapter. Watershed algorithm is employed to separate closed, touched and overlapped glistening. We avoid over-segmentation by extracting foreground of glistening before using watershed algorithm. As a result, the proposed algorithm has high effective.

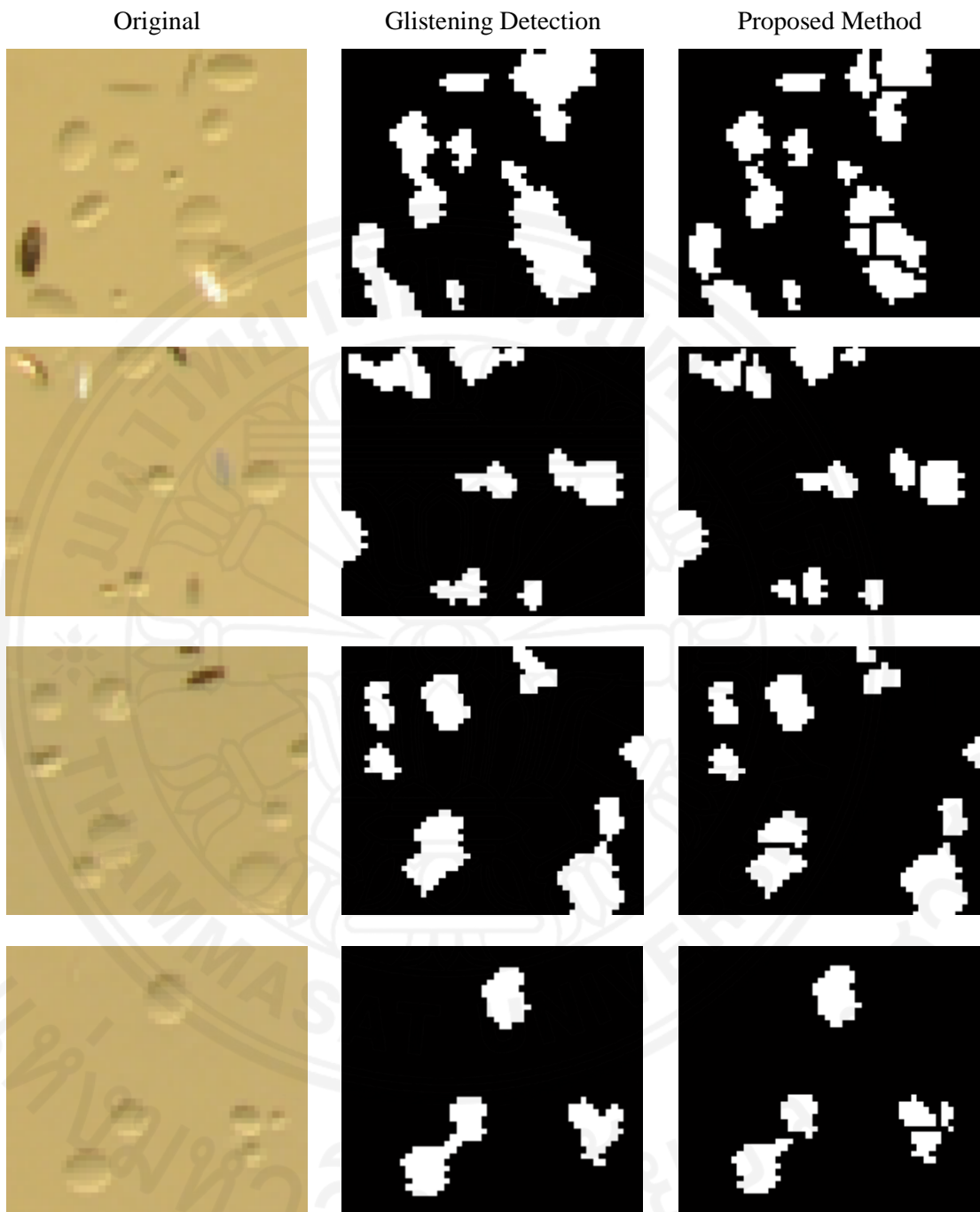


Fig. 4.4 Example of final result of Glistening separation algorithm (set 1)

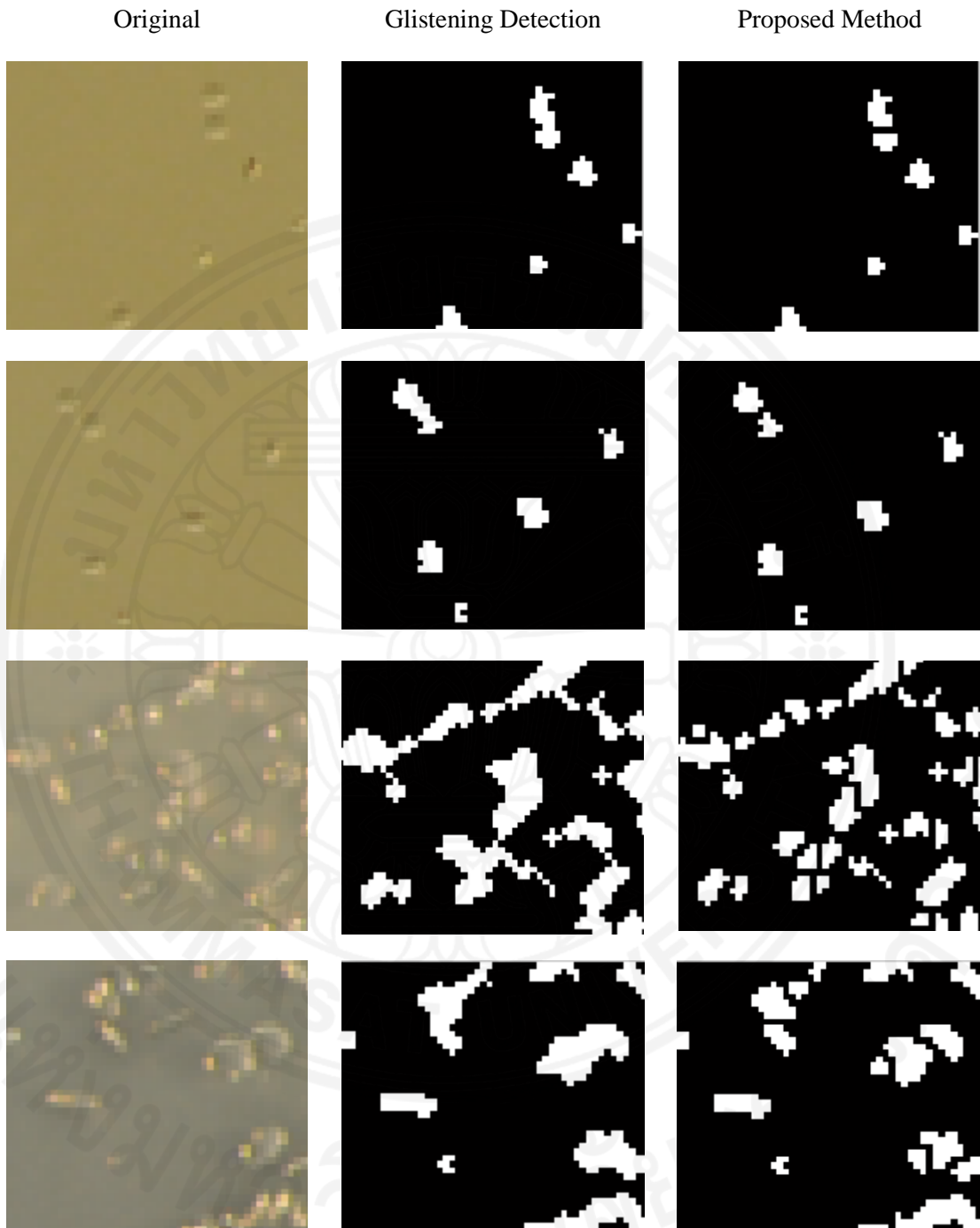


Fig. 4.5 Example of final result of Glistening separation algorithm (set 2)

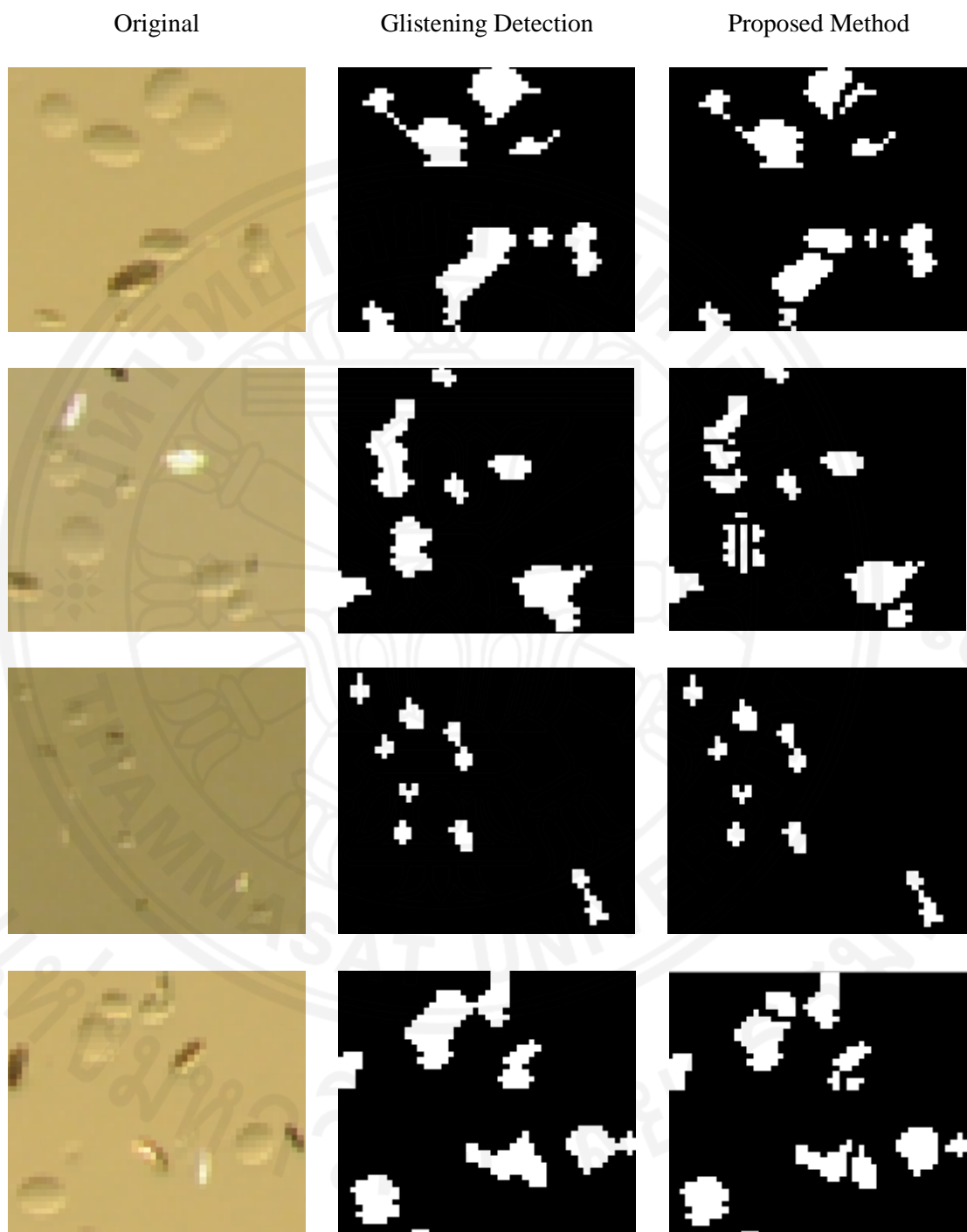


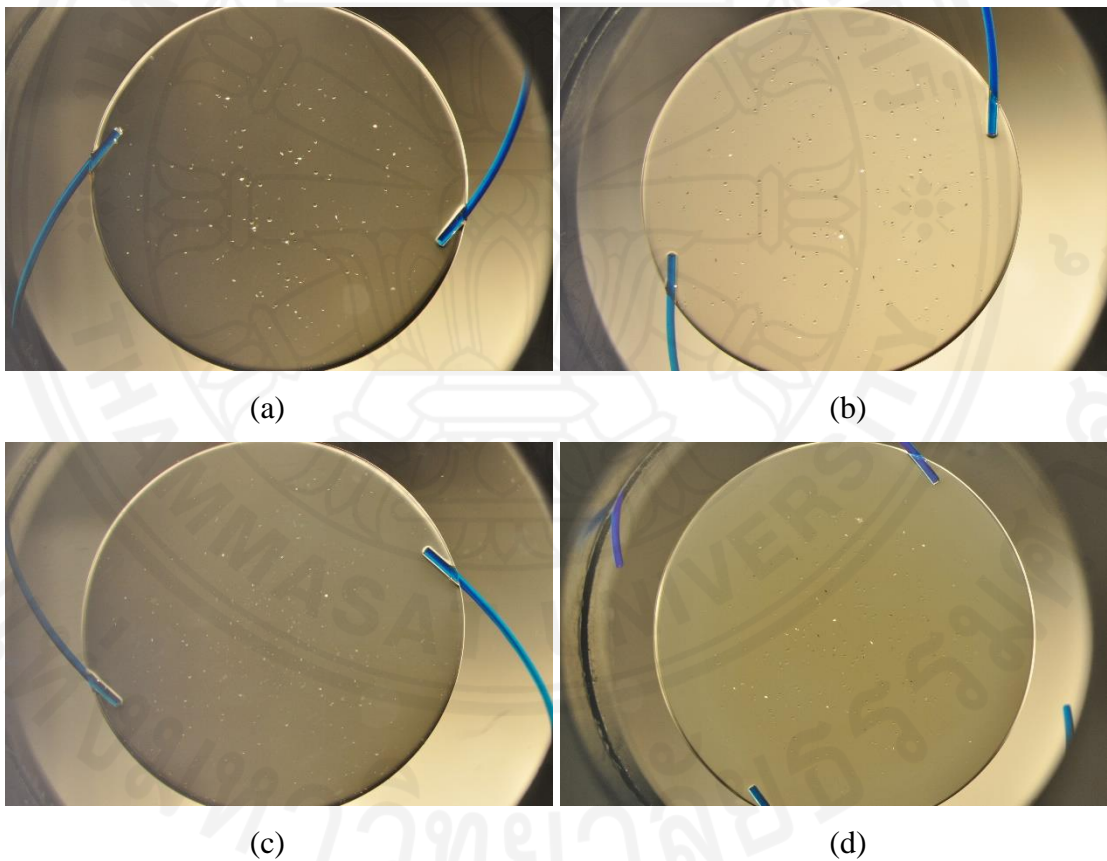
Fig. 4.6 Example of final result of Glistening separation algorithm (set 3)

Chapter 5

Evaluation and Result Discussion

5.1 Experimental Data

To evaluate the performance of the proposed technique, 20 input images obtained from the Applied Vision Research Centre, School of Health Sciences, City University London are used as a test set. The IOL input image is RGB color space. It has difference size and resolution. The environment of IOL image also difference. Fig. 4.1 shows several image of IOL input image.



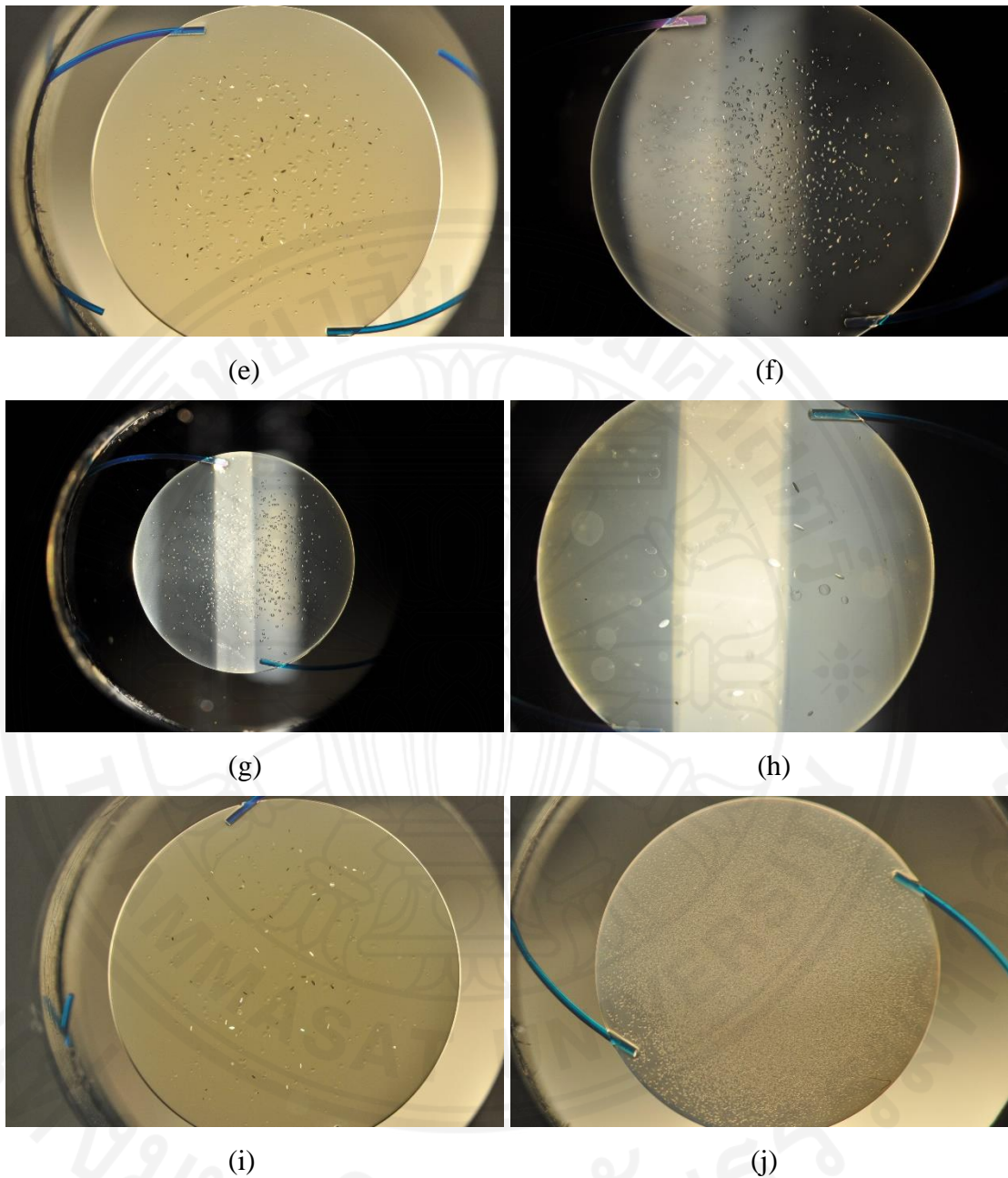


Fig. 5.1 Several images of IOL input image.

To evaluate the proposed algorithm, the ground truth from City University London is used. Firstly, the IOL image is marked with the red dot manually from the clinician. The example image is shown in Fig. 4.2 (a). After that, we have detected the red dot and change it into white while others area is black. Fig. 4.2 (b) shows the example image after ground truth is prepared for Glistening detection software.

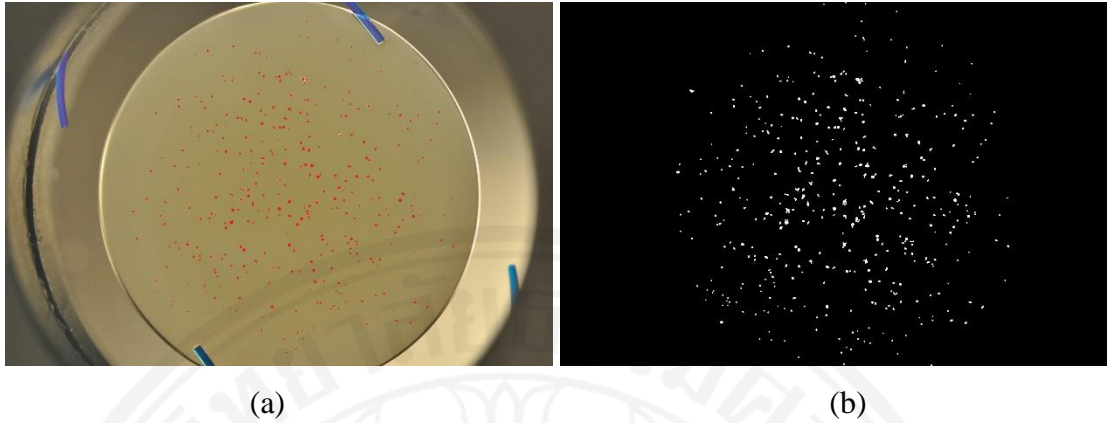


Fig. 5.2 Example of the ground truth image.

5.2 Evaluation

We have divided it into 2 big parts to evaluate the method. First, we will calculate accuracy and sensitivity of the method pixel-by-pixel. The second one, the number of glistening will be count blob-by-blob and compared with the ground truth.

5.2.1 Accuracy and Sensitivity

The accuracy and sensitivity are employed to compute performance of the glistening detection. The accuracy is the correct result divided by the total number of classifications of the pixel as define in Eq.2. Sensitivity is the true positive and the condition negative as defined in Eq. 3.

$$Accuracy = \frac{TP+TN}{TP+TN+FN+FP} \quad (2)$$

$$Sensitivity = \frac{TP}{TP+FN} \quad (3)$$

Table 5.1. Result of Glistening detection and variable data for each image.

Name #Image	Area of glistening		Threshold value			Accuracy	Sensitivity
	max	Min	Min	Max	Step	(%)	(%)
0326	0.09	0.0004	0.01	1	0.01	96.03	71.75
0390	0.09	0.001	0.01	1	0.01	94.64	75.85
0395	0.09	0.0002	0.02	1	0.01	98.08	59.62
0458	0.09	0.0005	0.01	1	0.02	97.76	76.64
0582	0.035	0.0001	0.02	1	0.01	99.51	62.52
0607	0.4	0.0001	0.02	1	0.01	98.67	56.38
0614	0.5	0.0001	0.03	1	0.02	99.33	78.38
0737	1	0.0001	0.01	1	0.01	99.38	71.72
0759	1	0.0002	0.01	1	0.02	98.82	86.93
0776	1	0.0002	0.02	1	0.02	98.38	87.07
0679	0.03	0.0005	0.03	1	0.01	99.58	49.44
0687	0.03	0.001	0.01	1	0.01	98.91	79.5
0692	0.03	0.0006	0.03	1	0.01	99.5	69.98
0699	0.03	0.0002	0.04	1	0.01	99.34	63.94
0723	0.055	0.0002	0.02	1	0.01	99.27	82.76
0728	0.055	0.0001	0.01	1	0.01	99.22	77.67
0734	0.055	0.0001	0.01	1	0.01	99.28	90.21
0740	0.03	0.001	0.01	1	0.01	99.1	99.38
0751	0.02	0.0001	0.02	1	0.01	99.45	70.6
0758	0.03	0.001	0.02	1	0.01	98.89	49.39
Average						98.66	72.98

Four types of result pixel are counted. True positive, TP, is a number of pixels which is correctly classified as glistening. False positive, FP, is a number of pixels which is wrongly classified as glistening. False negative, FN, is a number of pixels which is incorrectly classified as non-glistening and finally, True negative, TN, is a number of pixels which is correctly classified as non-glistenings.

The number of FP is quite large because some images have noise such as light which create some area shown like a light spot or dark spot in the input image.

In finally, the final result shows that our method has the good performance with the accuracy average of 98.66% and the sensitivity average of 72.99%.

5.2.2 Number of Glistening

From 20 images of test set, there are 9 images which have closed, touch and overlapped glistenings. However, 3 of the 9 images are hard to count although using human eye. Fig. 5.3 show the IOL image which hard to count. Thus, we can get only 6 images from all 20 images. Each image was divided into 25 images into the same size, so the set test consists of 150 images. Then, the number of glistening which is marked by the doctor will be counted to make a ground truth.

In 150 images, there are 57 images which have no glistening. Therefore, the subimage which is use in test set would be 93 images. Table 5.2 shows the number of Glistening separation method comparing with the ground truth.

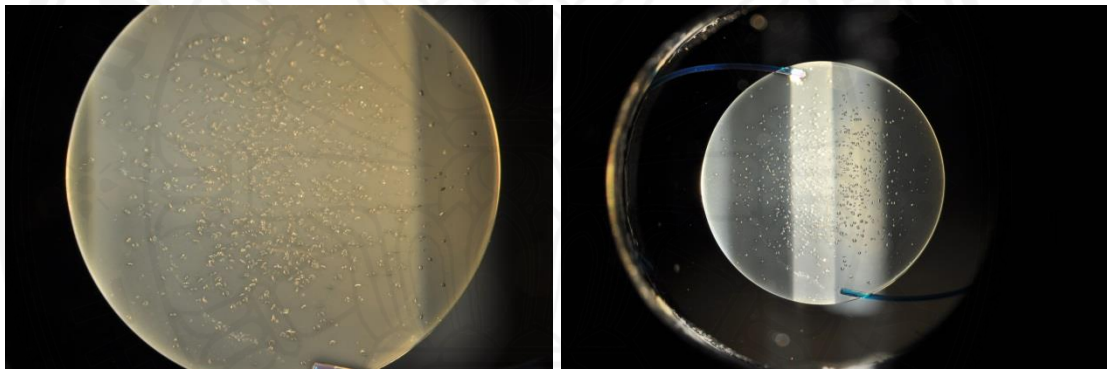


Fig. 5.3 Example of the IOL lens which hard to count glistening with human eye.

Table 5.2. Number of Glistening from the proposed method and ground truth.

No.	Proposed method	Ground Truth	Accuracy (%)
1	5	9	55.56
2	15	16	93.75
3	12	12	100
4	8	7	85.71
5	11	16	68.75
6	31	34	91.18
7	25	33	75.77
8	30	31	96.77
9	18	18	100
10	1	1	100
11	23	23	100

No.	Proposed method	Ground Truth	Accuracy (%)
12	26	26	100
13	29	20	55
14	9	8	87.5
15	2	2	100
16	25	33	75.75
17	37	39	94.87
18	28	31	90.32
19	5	6	83.33
20	15	19	78.95
21	66	70	94.29
22	70	70	100
23	63	64	98.44
24	25	37	67.57
25	9	16	56.25
26	35	46	76.09
27	43	46	93.48
28	42	48	87.5
29	9	16	56.25
30	3	4	75
31	0	0	100
32	3	2	50
33	17	20	85
34	21	30	70
35	19	30	63.33
36	7	18	38.89
37	9	13	69.23
38	38	42	90.48
39	52	54	96.30
40	34	39	87.18
41	19	27	70.37
42	3	6	50
43	20	23	86.96
44	34	39	87.18
45	23	35	65.71
46	15	18	83.33
47	6	6	100
48	8	8	100

No.	Proposed method	Ground Truth	Accuracy (%)
49	0	1	0
50	23	28	82.14
51	19	23	82.61
52	10	11	90.91
53	19	14	64.29
54	28	32	87.5
55	22	28	78.57
56	17	19	89.47
57	11	8	62.5
58	27	36	75
59	26	30	86.67
60	8	8	100
61	11	8	62.5
62	14	16	87.5
63	3	5	60
64	4	6	66.67
65	3	8	37.5
66	8	8	100
67	22	22	100
68	9	16	56.25
69	2	1	0
70	18	18	100
71	23	35	65.71
72	11	17	64.71
73	1	2	50
74	12	12	100
75	27	33	81.82
76	12	17	70.59
77	1	1	100
78	15	17	88.24
79	6	6	100
80	2	3	66.67
81	3	6	50
82	22	28	78.57
83	8	12	66.67
84	5	10	50
85	35	37	94.59

No.	Proposed method	Ground Truth	Accuracy (%)
86	15	21	71.43
87	1	1	100
88	13	13	100
89	25	27	92.59
90	13	14	92.86
91	1	1	100
92	5	12	41.67
93	3	6	50
Average			78.26

5.3 Conclusion

In this chapter, the result of Glistening detection is presented. To evaluate the proposed method, we have divided it into 2 parts, consists of Accuracy and Sensitivity part and number of glistening part.

In Accuracy and Sensitivity part, we calculate accuracy and sensitivity of this method by counting pixel-by-pixel. Using ground truth from City University London, the performance of this method is promising. The results show that accuracy is 98.01% and sensitivity is 72.67%.

In a number of glistening part, we counted a number of glistening which is marked in Ground truth. The result shows that, in counting method, the accuracy is 78.26%.

Chapter 6

Conclusions and Recommendations

This chapter is a brief describe the overall summary of this study. The key contributions and recommendations are explained towards the development for next research in the future.

6.1 Research Summary

Previously, studies of glistenings involved tedious work of manual glistenings labeling and rough estimation of glistening distribution. This research has studied the novel method to automatic glistening detection. The proposed method is blob-based and exudate-base detection. It also applied the watershed algorithm to increase performance in counting part and an average area of the glistening result. This method processes with Glistening detection program which designed by MATLAB. After user fill important data includes maximum glistening area, minimum glistening area, maximum threshold value, minimum threshold value, step threshold value and lens mark, the software computes and displays important properties such as average glistening area and distribution of glistening for user. All results in this program calculate from Glistening detection method. The result shows that the proposed method have a high performance for detect glistening. It can work with IOL images although it has a lot of noises. In case of overlapped, closed or touch glistenings, Watershed algorithm is applied to separate those glistenings. Thus, the results are more effectively.

6.2 Key Contributions of this Research

- a. Program efficiency of glistening detection designed by MATLAB.
- b. The novel method of automatic Glistening detection base on blob detection and exudate detection.
- c. Glistening separation developed by watershed algorithm.

6.3 Future Study

Glistening detection shows the result with high performance and it works with the noisy input image. It can also separate glistening which is touched, closed or

overlapped for more efficiently. However, glistening detection is provided a lot of time for computation because of the loop of difference thresholding value. It means if glistening have several of edge clarity and thresholding step is low, the process takes a lot of time to complete. In addition, the separation part, we employ Otsu's thresholding algorithm to extract foreground but glistenings have several of appearances such as white sesame, black sesame, and bubble. Therefore, in foreground extraction step, foreground image can extract only glistening whose white or black.

In future work, the algorithm of glistening can be improved for high-speed computation by apply recursive function. The recursive function is the function which can call itself. It can process one function in parallel. Thus, if we apply recursive function in Glistening detection algorithm, the computation time can be decreased.

In foreground extraction problem, we can change one thresholding value into two or several thresholding value. The result of each thresholding value can be combined for the better foreground image. With this idea, the number of glistening would be more accurate.

References

- [1] R. Bellucci, “An introduction to intraocular lenses: material, optics, haptics, design and aberration,” 2013.
- [2] L. Werner, “Glistenings and surface light scattering in intraocular lenses,” *Journal of Cataract & Refractive Surgery*, vol. 36, no. 8, pp. 1398 – 1420, 2010. [Online]. Available: <http://www.sciencedirect.com/science/article/pii/S0886335010008308>
- [3]. D. Tognetto, L. Toto, G. Sanguinetti, and G. Ravalico, “Glistenings in foldable intraocular lenses,” *Journal of Cataract & Refractive Surgery*, vol. 28, no. 7, pp. 1211 – 1216, 2002. [Online]. Available: <http://www.sciencedirect.com/science/article/pii/S0886335002013536>
- [4] N. Mamalis, “Intraocular lens glistenings,” *Journal of Cataract & Refractive Surgery*, vol. 38, no. 7, pp. 1119 – 1120, 2012. [Online]. Available: <http://www.sciencedirect.com/science/article/pii/S088633501200675X>
- [5] J. Colin, I. Orignac, and D. Touboul, “Glistenings in a large series of hydrophobic acrylic intraocular lenses,” *Journal of Cataract & Refractive Surgery*, vol. 35, no. 12, pp. 2121 – 2126, 2009. [Online]. Available: <http://www.sciencedirect.com/science/article/pii/S0886335009007822>
- [6] U. Gunenc, F. Oner, S. Tongal, and M. Ferliel, “Effects on visual function of glistenings and folding marks in acrysof intraocular lenses,” *Journal of Cataract & Refractive Surgery*, vol. 27, no. 10, pp. 1611 – 1614, 2001. [Online]. Available: <http://www.sciencedirect.com/science/article/pii/S0886335001009956>
- [7] E. Mnestam and A. Behndig, “Impact on visual function from light scattering and glistenings in intraocular lenses, a long-term study,” *Acta Ophthalmologica*, vol. 89, no. 8, pp. 724–728, 2011. [Online]. Available: <http://dx.doi.org/10.1111/j.1755-3768.2009.01833.x>
- [8] K. Hayashi, A. Hirata, M. Yoshida, K. Yoshimura, and H. Hayashi, “Long-term effect of surface light scattering and glistenings of intraocular lenses on visual function,” *American Journal of Ophthalmology*, vol. 154, no. 2, pp. 240 –

- 251.e2, 2012. [Online]. Available:
<http://www.sciencedirect.com/science/article/pii/S0002939412002024>
- [9] M. van der Mooren, L. Franssen, and P. Piers, "Effects of glistenings in intraocular lenses," *Biomed. Opt. Express*, vol. 4, no. 8, pp. 1294–1304, Aug 2013. [Online]. Available:
<http://www.opticsinfobase.org/boe/abstract.cfm?URI=boe-4-8-1294>
- [10] T. Japunya, P. Jitpakdee, B. Uyyanonvara, P. Aimmanee, E. Philippaki, C Hull, and Sarah Barman, "Software for the Quantification of Glistenings in Intra-Ocular Lenses," *The World Congress on Engineering 2014*, vol 1, 2014.
- [11] C. J and O. I, "Glistenings on intraocular lenses in healthy eyes: effects and associations," *Journal of Refractive Surgery (Thorofare,N.J. : 1995)*, pp. 869–875, 2011.
- [12] L. Wang and H. Ju, "A robust blob detection and delineation method," in *Education Technology and Training, 2008. and 2008 International Workshop on Geoscience and Remote Sensing. ETT and GRS 2008. International Workshop on*, vol. 1, Dec 2008, pp. 827–830.
- [13] Z. Qiu, L. Yang, and W. Lu, "A new featurepreserving nonlinear anisotropic diffusion for denoising images containing blobs and ridges," *Pattern Recognition Letters*, vol. 33, no. 3, pp. 319 – 330, 2012. [Online]. Available:
<http://www.sciencedirect.com/science/article/pii/S016786551100376X>
- [14] A. J. Danker, and A. Rosenfeld, "Blob Detection by Relaxation," *Pattern Analysis and Machine Intelligence, IEEE Transactions on* , vol.PAMI-3, no.1, pp.79,92, Jan. 1981
- [15] C. J and O. I, "Glistenings on intraocular lenses in healthy eyes:effects and associations," *Journal of Refractive Surgery (Thorofare, N.J. : 1995)*, pp. 869–875, 2011.
- [16] D. Youssef, N. Solouma, A. El-dib, M. Mabrouk, and A.-B. Youssef, "New feature-based detection of blood vessels and exudates in color fundus images," in *Image Processing Theory Tools and Applications (IPTA), 2010 2nd International Conference on*, July 2010, pp. 294–299.

- [17] Damerval, C.; Meignen, S., "Blob Detection With Wavelet Maxima Lines," *Signal Processing Letters, IEEE* , vol.14, no.1, pp.39,42, Jan. 2007 doi: 10.1109/LSP.2006.879830
- [18] L. Wang and H. Ju, "A robust blob detection and delineation method," in Education Technology and Training, 2008. and 2008 International Workshop on Geoscience and Remote Sensing. ETT and GRS 2008. International Workshop on, vol. 1, Dec 2008, pp. 827–830.
- [19] Inthajak, K.; Duanggate, C.; Uyyanonvara, B.; Makhanov, S.S.; Barman, S., "Medical image blob detection with feature stability and KNN classification," in Computer Science and Software Engineering (JCSSE), 2011 Eighth International Joint Conference on , vol., no., pp.128-131, 11-13 May 2011 doi: 10.1109/JCSSE.2011.5930107
- [20] Waseem, S.; Akram, M.U.; Ahmed, B.A., "Drusen detection from colored fundus images for diagnosis of age related Macular degeneration," in Information and Automation for Sustainability (ICIAfS), 2014 7th International Conference on , vol., no., pp.1-5, 22-24 Dec. 2014 doi: 10.1109/ICIAFS.2014.7069581
- [21] Huiying Liu; Yanwu Xu; Wong, D.W.K.; Jiang Liu, "Growcut-based drusen segmentation for age-related macular degeneration detection," in Visual Communications and Image Processing Conference, 2014 IEEE , vol., no., pp.161-164, 7-10 Dec. 2014 doi: 10.1109/VCIP.2014.7051529
- [22] Bhuiyan, A.; Karmakar, C.; Di Xiao; Ramamohanarao, K.; Kanagasingham, Y., "Drusen quantification for early identification of age related macular degeneration (AMD) using color fundus imaging," in Engineering in Medicine and Biology Society (EMBC), 2013 35th Annual International Conference of the IEEE , vol., no., pp.7392-7395, 3-7 July 2013 doi: 10.1109/EMBC.2013.6611266
- [23] Yifei Zhang; Shuang Wu; Ge Yu; Daling Wang, "A Hybrid Image Segmentation Approach Using Watershed Transform and FCM," *Fuzzy Systems and Knowledge Discovery, 2007. FSKD 2007. Fourth International Conference on* , vol.4, no., pp.2,6, 24-27 Aug. 2007

- [24] Li Cheng; Li Yan; Fan Shangchun, "CCD Infrared Image Segmentation Using Watershed Algorithm," Measuring Technology and Mechatronics Automation (ICMTMA), 2011 Third International Conference on , vol.1, no., pp.680,683, 6-7 Jan. 2011.
- [25] K. Parvati, B. S. Prakasa Rao, and M. Mariya Das, —Image Segmentation Using Gray-Scale Morphology and Marker-Controlled Watershed Transformation, Discrete Dynamics in Nature and Society, vol. 2008, Article ID 384346, 8 pages, 2008
- [26] Jun Tang, "A color image segmentation algorithm based on region growing," Computer Engineering and Technology (ICCET), 2010 2nd International Conference on , vol.6, no., pp.V6-634,V6-637, 16-18 April 2010
- [27] Wei Zhang; DaLing Jiang, "The marker-based watershed segmentation algorithm of ore image," Communication Software and Networks (ICCSN), 2011 IEEE 3rd International Conference on , vol., no., pp.472,474, 27-29 May 2011
- [28] Yinghong Liu; Qingjie Zhao, "An improved watershed algorithm based on multi-scale gradient and distance transformation," Image and Signal Processing (CISP), 2010 3rd International Congress on , vol.8, no., pp.3750,3754, 16-18 Oct. 2010
- [29] Yifei Zhang; Shang Wu; Ge Yu; Daling Wang, "Medical Image Segmentation Based on Fast Region Connecting," Complex Medical Engineering, 2007. CME 2007. IEEE/ICME International Conference on , vol., no., pp.833,836, 23-27 May 2007
- [30] Xiaodong Zhang, Fucang Jia, Suhuai Luo, Guiying Liu, Qingmao Hu, A marker-based watershed method for X-ray image segmentation, Computer Methods and Programs in Biomedicine, Volume 113, Issue 3, March 2014, Pages 894-903
- [31] Rahman, M.H.; Islam, M.R., "Segmentation of color image using adaptive thresholding and masking with watershed algorithm," Informatics, Electronics & Vision (ICIEV), 2013 International Conference on , vol., no., pp.1,6, 17-18 May 2013

Appendix A
List of Publication

1. T. Japunya, P. Jitpakdee, B. Uyyanonvara, P. Aimmanee, E. Philippaki, C Hull, and Sarah Barman, “Software for the Quantification of Glistenings in Intra-Ocular Lenses,” The World Congress on Engineering 2014, vol 1, 2014.
2. T. Japunya, P. Jitpakdee, B. Uyyanonvara, C. Sinthanayothin, and H. Kaneko, “Quantification of the overlapped Glistening in Intraocular lens,” The 5th International Congress on Engineering and Information 2015, May 2015.
3. T. Japunya, P. Jitpakdee, B. Uyyanonvara, C. Sinthanayothin, and H. Kaneko, “Automatic blob-based Glistening Detection,” 2015 International Symposium Multimedia and Communication Technology September 23 – 25, 2015,